Copy 93
RM E51C29

NACA

RESEARCH MEMORANDUM

EXPERIMENTAL INVESTIGATION OF AIR-COOLED TURBINE BLADES IN TURBOJET ENGINE

VI - CONDUCTION AND FILM COOLING OF LEADING AND TRAILING EDGES OF ROTOR BLADES

By Vernon L. Arne and Jack B. Esgar

Lewis Flight Propulsion Laboratory
Cleveland, Ohio

NATIONAL ADVISORY COMMITTEE
FOR AERONAUTICS

WASHINGTON

May 18, 1951

NACA RM E51C29

NATIONAL ADVISORY COMMITTEE FOR AERONAUTICS

RESEARCH MEMORANDUM

EXPERIMENTAL INVESTIGATION OF AIR-COOLED TURBINE BLADES IN TURBOJET ENGINE VI - CONDUCTION AND FILM COOLING OF LEADING AND TRAILING EDGES OF ROTOR BLADES

By Vernon L. Arne and Jack B. Esgar

SUMMARY

A series of four air-cooled turbine-blade configurations was investigated as part of a program to develop air-cooled turbine-blade configurations fabricated from nonstrategic materials that are capable of sustained operation at current inlet-gas temperatures. The results of this investigation are presented and compared with other blade configurations previously investigated.

The values of blade-cooling effectiveness and pressure-loss parameter were determined over a range of engine speed from 4000 to 10,000 rpm and a range of cooling-air flow from about 0.03 to about 0.10 pound per second per blade.

The configurations presented were investigated in order to evaluate modifications of promising blade-cooling schemes indicated by previous similar investigations. The use of a high-conductivity metal coating on the inner surface of the blade wall was effective in further reducing the temperature gradients on the blade. The use of a double-flow cooling-air path on the film-cooled blades improved the cooling-air pressure loss in relation to the original reverse-flow film-cooled blade.

The use of a single row of large leading-edge slots in place of the previously investigated three-row arrangement resulted in equally effective leading-edge cooling and provided a more structurally rigid leading-edge section; however, the film-cooling flow was unstable so that the division of flow over the pressure and suction surfaces was often unpredictable.

At an engine speed of 10,000 rpm, an effective gas temperature of 1070° F, a coolant- to gas-flow ratio of 0.0534, and a cooling-air inlet temperature at the blade root of 130° F, the temperatures of the leading edges of a copper-clad blade, a film-cooled blade with three rows of radial leading-edge slots, and a film-cooled blade with a single row of radial leading-edge slots were 850°, 780°, and 720° F, respectively; the average midchord temperatures were about 660°, 635°, and 660° F, respectively; and the trailing-edge temperatures were 720°, 670°, and 610° F, respectively. The film-cooled type of blade exhibited a rapid loss in leading- and trailing-edge cooling effectiveness below certain coolant-flow rates so that the preceding comparison may be altered in favor of internal convection-cooled blade types, such as the copper-clad blade, at lower coolant-flow rates.

INTRODUCTION

An investigation is being conducted at the NACA Lewis laboratory to determine means of air-cooling turbine blades to reduce the strategic-metal content in turbojet and turbine-propeller engines. The results of earlier phases of this investigation are reported in references 1 to 5. The first three blade configurations investigated (references 1 to 3) established that blade designs consisting of hollow blade shells containing tubes and fins were effectively cooled at the midchord positions but were as much as 500° hotter at the leading and trailing regions of the blade. Calculations of allowable turbine-inlet temperatures for nonstrategic blades based on measured data from these three blade configurations indicated that the high leading- and trailing-edge temperatures may limit the operation of such nonstrategic blades to inlet temperatures below those in current use.

In order to reduce the high chordwise temperature gradients found in the first three blade configurations, a series of seven blade designs incorporating special means of cooling the leading- and trailing-edge regions of the blades was investigated (references 4 and 5). A blade utilizing high-conductivity tubes and fins to conduct heat away from the leading and trailing edges and a blade employing a reverse-flow coolant path and with film-cooled leading and trailing edges were found to have blade-temperature distributions that indicate they are capable of operation at current turbine-inlet temperatures when fabricated from nonstrategic materials.

The blade utilizing high-conductivity (copper) fins and tubes (reference 4) was difficult to fabricate and some difficulty was encountered in maintaining a good thermal bond between the copper and the blade shell. In order to increase the conductivity of the entire blade

shell rather than just the leading and trailing edges and to simplify the blade fabrication, a blade consisting of a copper-clad shell with seven copper tubes in the midchord was investigated.

The reverse-flow blade (reference 4) exhibited a spanwise temperature profile where the temperatures decreased from root to tip and the coolant pressure losses were high. Because the allowable blade temperature usually increases from root to tip, the spanwise temperature profile of the reverse-flow blade is undesirable. In an effort to alter this temperature profile and also to improve the coolant pressure losses, a double-flow blade was fabricated so that part of the cooling air could flow directly from the base of the blade into the leading- and trailing-edge passages that supply air to the film-cooling slots. The remainder of the air flowed through tubes in the midchord region and then reversed flow direction at the tip in order to enter the leading- and trailing-edge supply passages, similar to the flow path of all the air in the reverse-flow blade.

The heat-transfer and pressure-loss results of the copper-clad blade and three versions of the double-flow blade are presented herein. The blades were investigated over a range of engine speeds from 4000 to 10,000 rpm and over a range of cooling-air-flow rates per blade from about 0.03 to 0.10 pound per second.

SYMBOLS

The following symbols are used in this report:

N	engine speed, (rpm)
p	static pressure, (in. Hg absolute)
p'	total pressure, (in. Hg absolute)
r	radius from center of rotor, (ft)
T	static temperature, ($^{\circ}F$)
T'	total temperature, ($^{\circ}F$)
w_a	cooling-air flow per blade, (lb/sec)
w_g	combustion-gas flow per blade, (lb/sec)

Y pressure-drop parameter, rotor hub to blade tip,

$$\frac{\rho_{a,H}}{\rho_0}\left[p'_{a,H} - \left(p'_m - \frac{\eta\omega^2 r_T^2 \rho_{a,H}}{70.7}\right)\right], \text{ (in. Hg)}$$

Y_1 pressure-drop parameter, blade root to blade tip,

$$\frac{\rho_{a,H}}{\rho_0}\left\{\left[p'_{a,H} - \left(p'_m - \frac{\eta\omega^2 r_T^2 \rho_{a,H}}{70.7}\right)\right] - \left(p_{a,H} - p_{a,h}\right)\right\}, \text{ (in. Hg)}$$

η efficiency of compression in turbine rotor

ρ density, (slugs/cu ft)

φ temperature-difference ratio, $(T_{g,e} - T_B)/(T_{g,e} - T_{a,e,h})$

ω angular velocity of rotor, (radians/sec)

Subscripts:

A combustion air

a blade-cooling air

B cooled blade

c compressor

e used to denote effective temperature

g combustion gas

H hub of rotor

h root of blade

i inlet

m mixture of combustion gas and scavenge, bearing, and blade-cooling air in tail pipe

T blade tip

0 NACA standard sea-level conditions

DESCRIPTION OF BLADES INVESTIGATED

The blades investigated in this report are designated blades 11, 12, 13, and 14. The shell of blade 11 was formed from copper-clad Inconel sheet, whereas the shells of the double-flow blades 12, 13, and 14 were cast from a high-temperature alloy, X-40. A summary of the pertinent features of the blade geometry and leading- and trailing-edge modifications is given in table I. A more detailed description of each of the blades follows.

Blade 11

Results of tests of a blade with copper tubes and with copper fins extending from the tubes to the leading and trailing edges are presented in reference 4. The results indicate that the design has good possibilities of combining the desirable properties of strength, cooling effectiveness, and low cooling-air pressure drop. In order to increase the conductivity of the blade shell and decrease fabrication difficulties encountered with the copper tube and fin blade, a copper-clad blade shown in figure 1 was investigated. The blade shell was formed from copper-clad Inconel sheet that was rolled into a tube having a tapered wall thickness. The tube was seam-welded and then stamped into the proper blade shape by means of formed dies. The thickness of the copper was 0.020 inch from blade root to tip, but the over-all thickness of the blade wall tapered from 0.070 inch at the root to 0.040 inch at the tip. The blade shell was packed with seven copper tubes having an outside diameter of 0.188 inch and a wall thickness of 0.032 inch. The tubes were brazed to the shell with a copper-silver eutectic.

Blades 12 and 13

Results of an investigation of reverse-flow blades (blades 7 and 8), which utilized film cooling and the forces of natural convection to help cool the leading and trailing edges of the blades, are reported in reference 4. All the cooling air passed radially outward through tubes contained in the central part of the blade, made a 180° turn at the blade tip, and then flowed out through leading- and trailing-edge slots as it flowed radially inward. These blades had a very favorable chordwise temperature profile, but they also had high pressure drops. In

addition, the trailing edge was substantially higher in temperature near the root than near the tip. This situation is undesirable because the maximum stress usually occurs at the blade root and decreases with increasing radius. Refinement in design of the trailing-edge slot to force more of the cooling air out near the root section would improve this situation, but it would make the coolant pressure drop even higher.

The purposes of fabricating blade 12 were to investigate a special means of cooling the root section of a blade similar to the reverse-flow blade and to reduce the coolant pressure losses. The central part of the blade and the leading- and trailing-edge sections of the half of the blade nearer the tip were cooled in the same way as blades 7 and 8 of reference 4. In blade 12, the leading- and trailing-edge passages were open at the root so that part of the cooling air could flow directly from the blade base to the leading- and trailing-edge passages and then out through the film-cooling slots in the half of the blade nearer the root. The air flowing in at the root and the tip of the leading- and trailing-edge passages was restrained to the lower and upper halves of the blade by dams that were placed in the leading- and trailing-edge passages at 50-percent span, as shown in figure 2. The leading-edge configuration contained three rows of 0.010-inch-wide radial slots, just as did the leading edges of blades 7 and 8 of reference 4. Blade 12, however, had a sharp leading edge, whereas blades 7 and 8 had rounded leading edges. The trailing edge contained a continuous slot 0.025 inch wide similar to the trailing-edge slot of blade 8, but in blade 12 the slot was interrupted at midspan by the dam in the trailing-edge passage. Nine stainless-steel tubes were packed and Nicrobrazed into the coolant passage. Five tubes had an outside diameter of 0.156 inch and a wall thickness of 0.020 inch, and the other four tubes had an outside diameter of 0.125 inch and a wall thickness of 0.018 inch.

Two blades of this configuration were fabricated and instrumented and heat-transfer tests were made at a number of engine speeds. The dams in the leading- and trailing-edge passages were then removed from the blade instrumented for the spanwise variation in temperature. This modification was made to determine if the dams had any effect on the cooling-air distribution and therefore on the spanwise temperature distribution at the leading and trailing edges. The blade with the dam removed is designated blade 13. Blades like 12 and 13 with flow into leading- and trailing-edge passages from both root and tip are called double-flow blades herein.

Blade 14

Blades with multiple rows of radial film-cooling slots at the leading edge have shown a tendency to develop cracks between adjacent slots. This tendency is believed to be due to vibrational stresses. In an effort to alleviate the susceptibility to crack formation, a blade with a single row of leading-edge slots was investigated. After the investigation was completed on blades 12 and 13, two of the rows of leading-edge slots were welded shut and the center row of slots was opened up to 0.020-inch width, as shown in figure 3. The leading- and trailing-edge dams were retained in the blade, which was instrumented for chordwise-temperature-distribution measurements. The blade instrumented for the spanwise-temperature-distribution measurements contained no dams, however, in order that the results from blade 14 would be directly comparable with those from blade 13.

APPARATUS AND INSTRUMENTATION

Engine

The turbojet engines used for this investigation were modified and instrumented in the same manner as the engines described in references 1 and 2. Provision was made for measuring the cooling-air flow, engine mass flow, engine speed, fuel flow, and compressor-inlet and -outlet temperatures and pressures.

Cooled Blades

The method of attaching the thermocouple leads to the blade shells was that used for previous investigations and consisted in placing a 0.040-inch Inconel tube containing the two thermocouple leads encased in two-hole ceramic tubing in a groove in the blade shell. A 0.020-inch wire was then spot-welded along each edge of the groove; this groove was covered with a commercial brazing alloy on blades 12, 13, and 14. A high-temperature paint was used on blade 11 because the brazing temperature was higher than the temperature used for bonding the copper tubes to the copper lining of the blade shell.

The locations of the thermocouples on the blades of this investigation are shown in figure 4. The instrumentation follows the general pattern established in previous investigations; one cooled blade gives a chordwise profile at approximately the one-third span position, and the other cooled blade, diametrically opposite, gives a spanwise distribution.

A thermocouple was located on the leading edge of an uncooled blade adjacent to each cooled blade at approximately the one-third span position in order to measure the effective gas temperature (thermocouples F and L). The cooling-air inlet temperature at the blade roots was measured by thermocouples E and K.

On blade 11 (fig. 4(a)), trailing-edge thermocouples were located at the one-third span location on both blades investigated so that the uniformity of the thermal bond between the copper coating and the Inconel blade shell could be checked at these locations. Thermocouples A, C, and D provided the spanwise profile and thermocouples G, H, I, J, and P provided the chordwise temperature distribution.

Blades 12 and 13 (fig. 4(b)) were instrumented to check the spanwise temperature profiles near both the leading and trailing edges. Thermocouples A, V, and C provided the trailing-edge profile; thermocouples T and U provided the leading-edge profile. Thermocouple V was located directly downstream of the trailing-edge dam so that the maximum trailing-edge temperature would be determined. Thermocouples G, J, H, and C provided the chordwise temperature profiles.

In order to evaluate the cooling effectiveness of the single-slot, film-cooled leading edge of blade 14 (fig. 4(c)), leading-edge thermocouples G and Q were installed on the suction and pressure surfaces near the leading edge symmetrical with the leading-edge slot. The distribution of cooling air on each surface could be inferred from this instrumentation. The chordwise temperature profile was determined by thermocouples G, H, C, J, and Q, and thermocouples A, C, T, and U provided the spanwise temperature distribution near the trailing and leading edges of the blade.

PROCEDURE

Experimentation

The procedure followed in conducting the experimental runs was the same as that followed in previous investigations (references 1 to 5). In general, a series of runs was made at various engine speeds for each

blade configuration. At each engine speed, the blade cooling-air flow was varied by remotely controlled valves in the cooling-air supply lines. Two series of runs were made at each engine speed because the rotating thermocouple pickup limited to six the number of thermocouples that could be read during each run.

A summary of the engine operating conditions is presented in table II; each of the parts (a), (b), (c), and (d) of the table applies to a particular blade configuration.

Calculations

The calculation procedures used for this report are also the same as those used in the previous reports of this series of cooled-turbine-blade investigations. In order to compute blade temperatures for conditions of gas and coolant temperature different from the data points, use was made of the nondimensional temperature-difference ratio φ. This ratio, $\varphi = (T_{g,e} - T_B)/(T_{g,e} - T_{a,e,h})$, was shown to be, for a given blade configuration, essentially a function of the combustion-gas- and cooling-air-flow rates (reference 1). Thus a plot of φ against coolant flow for different gas flows makes possible a calculation of blade temperature T_B for any gas and coolant temperature over the range of coolant and combustion-gas flows plotted. Because blade temperatures can be calculated in this way, curves of blade temperature can be determined for a wide range of engine conditions. These curves permit the calculation of allowable turbine-inlet temperatures by determination of the spanwise-blade-temperature distribution that is tangent to the allowable blade temperature for the particular blade configuration. This method is presented in detail in reference 1.

The method for correlating the cooling-air pressure loss through the blade is discussed in references 2 and 3.

RESULTS AND DISCUSSION

The blades investigated were designed with intent to improve the heat-transfer and pressure-loss characteristics of two of the promising blade configurations previously investigated (reference 4). The results of the copper-clad blade (blade 11) and the double-flow blades (blades 12, 13, and 14) are compared with the copper-fin blade (blade 9) and the reverse-flow blade (blade 8) from reference 4 in the following paragraphs.

Observed Blade Temperatures

In figures 5 to 8, the blade temperatures are presented as they were observed for the highest engine speed at which data were taken during the investigation for each blade configuration; these conditions were the most severe and represented the nearest approach during the investigation to conditions that would be realized in an actual engine application. As expected, a decrease in cooling-air flow was accompanied by an increase in cooled-blade temperature for all thermocouple locations. Comparison of temperatures for leading-edge thermocouple G for blades 11 and 12 (figs. 5(a) and 6(a)) shows that the leading-edge temperature increases more rapidly as coolant flow is decreased for the film-cooled leading-edge blade 12, than for the copper-clad blade 11. This effect has been observed for slotted film-cooled blades (reference 4) and indicates a flow rate for film-cooled leading edges of this type below which a rapid increase in leading-edge temperature results. Blade 14, which has a single row of leading-edge slots, shows a similar characteristic for thermocouple readings on both sides of the slot. Thermocouple Q of figure 8(a) is on the pressure side of the blade and thermocouple G is on the suction side. Thermocouple Q showed a temperature over 250° higher than thermocouple G for most of the range, and indicated that the flow out of the slot divided unequally with more of the coolant flow covering the suction surface. This characteristic of the single-slot type of blade is undesirable because the division of flow may be quite sensitive to angle of attack and flow conditions over the outside of the blade, and therefore prediction of the cooling effectiveness at conditions other than those of the investigation or for spanwise locations other than the particular one measured is difficult.

Leading- and trailing-edge temperatures were taken at two spanwise positions on the film-cooled blades. Figure 6(b) shows the temperatures measured for a double-flow blade (blade 12) at 8000 rpm, which was the highest speed tested with this thermocouple grouping on blade 12. Thermocouple A (near the blade tip) is from 75° to 100° F hotter than C (near one-third span) at the trailing edge and thermocouple T (near tip) is about 150° hotter than U (near one-fourth span) at the leading edge over most of the range of coolant flow. In figure 7, the same thermocouple readings are shown at 10,000 rpm for blade 13, which is the same as blade 12 with the dams removed. Thermocouple A is still over 100° hotter than C, but thermocouple T at the leading edge has now cooled about 200° below thermocouple U, indicating a greater coolant flow out the leading edge in the section of the blade near the tip. The results from figures 6(b) and 7 are not directly comparable because they are for different engine speeds, and as will be shown, the effect of engine speed on the spanwise temperature

distribution can be appreciable. The leading- and trailing-edge temperatures for blade 14 are shown in figure 8(b). Here the temperatures are about 30° higher near the blade root than near the tip over most of the cooling-air-flow range investigated. At low flows, thermocouple T increases rapidly in temperature, indicating that the film cooling is beginning to break down over that portion of the blade.

Because of difficulty in maintaining a uniform thermal bond between the copper tubes and the alloy shell of the blade (reference 4), thermocouples I and C were located in similar positions on the two blades of configuration 11 to determine if a variation in the bonding between the alloy shell and the copper lining was present. A comparison of the results of the variation of blade temperatures at locations C and I with cooling-air-flow rate (figs. 5(a) and 5(b)) shows these two positions to have a negligible temperature difference over the entire range of cooling-air flow investigated; consequently, it is apparent that no appreciable variation of the thermal bond was present at this location.

Correlation of Blade Temperatures

The method of correlating the measured blade temperatures is given in reference 1. The nondimensional temperature-difference ratio

$$\varphi = \frac{T_{g,e} - T_B}{T_{g,e} - T_{a,e,h}}$$

is shown to be mainly a function of coolant flow w_a and hot gas flow w_g for an air-cooled blade. Good correlation for all engine speeds investigated was obtained when φ was plotted against the ratio of w_a to w_g, as illustrated in figure 9(a) for blade 11 at the midchord thermocouple J. The correlation at the leading-edge thermocouple G was poorer (fig. 9(b)). This change is believed to be caused by a change in angle of attack as engine speed is changed. The effect of this change is therefore much more noticeable at the leading edge than at the midchord because the angle of attack has little effect on the flow in the passage between the blades.

Values of φ for all thermocouple positions for all blades investigated at three engine speeds are given in table II.

Comparison of Blade Temperatures

Chordwise temperature distribution. - By use of the data of the previous figures, chordwise variations of temperature at the one-third span position were drawn. Blades 11, 12, and 14 were compared at two values of coolant-flow ratio at 10,000 rpm because the film-cooled blades tend to be well cooled at the high flows; however, the cooling effectiveness rapidly drops off as the coolant flow is decreased. The coolant-flow ratio is defined as the ratio of coolant flow per blade to hot gas flow per blade and values of 0.045 and 0.0534 were selected. These values correspond to measured points for the copper-clad blade. For the other blades, which had slightly different gas and coolant temperatures, the blade temperatures were calculated from values of the temperature-difference ratio φ taken from faired curves.

A comparison of the chordwise temperature distribution at a coolant-flow ratio of 0.0534, an effective gas temperature of 1070° F, and a cooling-air inlet temperature at the blade root of 130° F, is shown in figure 10(a) for the blades investigated. No chordwise distribution was sought for blade 13 as removal of the dam in the blade was expected to affect mainly the spanwise distribution of leading- and trailing-edge temperature, and any small variations in midchord temperature would have little effect on the evaluation of the effectiveness of dams in giving more desirable spanwise temperature. At a coolant-flow ratio of 0.0534, the leading-edge temperatures of blade 11, blade 12, and blade 14 were 850°, 780°, and 720° F, respectively; the average midchord temperatures were about 660°, 635°, and 660° F, respectively; and the trailing-edge temperatures were 720°, 670°, and 610° F, respectively. Blade 11 has a leading-edge temperature 215° higher than its lowest midchord temperature and a trailing-edge temperature only about 90° higher than its lowest midchord temperature. The film-cooled blade with three leading-edge slots (blade 12) has a leading-edge temperature 170° higher and a trailing-edge temperature about 65° higher than its lowest midchord temperature. Blade 14, with a single leading-edge slot, exhibits an unusual leading-edge characteristic with the temperature on a suction side of the leading-edge slot about 300° cooler than on the pressure side of the slot, a fact that indicates uneven division of the cooling air over the blade. This flow division is sometimes unstable, as was evidenced by some runs repeated during the course of the investigation. In these runs, the temperature on the suction side of the slot increased and the temperature on the pressure side of the slot decreased, indicating a change in the division of coolant flow. The cooled blades used in this investigation were untwisted and, consequently, there is a variation in the angle of attack of the cooled blades with span. It is therefore possible that the division of flow from the leading-edge slot varies with span.

Blades 11, 12, and 14 are compared at a coolant-flow ratio of 0.045 in figure 10(b). This small reduction in coolant flow gives a definite increase in temperature for the film-cooled blades, indicating that this coolant flow is in a critical region where the film cooling tends to break down. Blade 12 shows this effect quite markedly. With this comparatively small change in coolant flow, the leading-edge temperature of blade 12 increased from 780° to about 950° F and the trailing-edge temperature increased from 670° to 830° F. The copper-clad blade (blade 11) showed only a 20° to 30° increase in these regions.

In figure 11, blade 11 is compared with previously tested blades at the coolant-flow ratio of 0.045. The maximum chordwise temperature gradient of 210° F in the copper-clad blade is a large improvement over the 470° F gradient in the 10-tube blade from reference 1. The lowest temperature gradient of the previously tested blades was blade 8, a film-cooled, reverse-flow blade reported in reference 4. As shown in figure 11, blade 8 has a temperature gradient of about 240° F at a coolant-flow ratio of 0.045. Also shown in figure 11 is the chordwise distribution for blade 9, which has copper tubes with copper fins extending from the tube bank to the leading and trailing edges. The investigation of this blade is also reported in reference 4. Blades 9 and 11 have approximately the same leading-edge temperatures and the copper-clad blade has a trailing-edge temperature about 80° cooler than the trailing edge of the copper-fin blade. The copper-clad blade shows lower leading- and trailing-edge temperatures at the expense of higher midchord temperatures.

The absence of large temperature gradients in the copper-clad blade, a condition that will reduce thermal stresses and localized overheating at the leading and trailing edges, will possibly compensate for the increased temperatures at the midchord section of the blade; however, the final evaluation of the various blade designs will depend upon systematic endurance investigations.

Spanwise temperature distribution. - The determination of an optimum spanwise temperature distribution is dependent on the establishment of an allowable temperature curve. The allowable temperature curve is dependent on the blade stresses and the elevated-temperature strength properties of the material. Allowable-temperature curves based on the radial stresses caused by centrifugal force almost always show lower allowable temperatures near the root; therefore it is desirable to have a temperature profile with as low an average temperature as possible and with the lowest temperature at the blade root.

Little can be done to control the spanwise temperature distribution of convection-cooled blades such as blade 11. In general, the spanwise temperature distribution is similar to the gas-temperature profile for this type of blade except that the cooling will be somewhat less effective near the blade tip because the cooling air heats up as it passes through the blade. From table II(a), it can be seen from the temperature-difference ratio φ for the trailing-edge thermocouples A, C, and D that for speeds of 4000 and 6000 rpm the blade is coolest at the root and hottest at the tip, the desired temperature profile; but as the speed is increased to 10,000 rpm, the hottest portion of the blade is at approximately 35-percent span. The portion of the blade near the root, however, is still the coolest.

By the proper introduction of the cooling air and control of slot size, it should be possible to control the spanwise temperature distribution on film-cooled blades at the leading and trailing edges. The reverse-flow blade 8 (references 4 and 5) was coolest near the blade tip and hottest near the blade root, an undesirable characteristic. The double-flow blades (12, 13, and 14) were designed with the intent to provide more effective cooling near the blade root. These efforts were only partly successful. From the values of φ for the leading-edge thermocouples T and U and the trailing-edge thermocouples A and C on tables II(b), (c), and (d) and from the temperatures on figures 6(b), 7, and 8(b), it can be seen that:

1. As shown in table II(b), the leading edge of blade 12 is hotter towards the tip than towards the base at all speeds investigated (up to 8000 rpm).

2. At 4000 and 6000 rpm (table II(b)), there is no definite trend in the spanwise temperature distribution at the trailing edge of blade 12; but at 8000 rpm, the blade is cooler at the root than at the tip, which is a desirable temperature profile.

3. Removal of the dams in the leading and trailing edges of blade 12 to make blade 13 apparently caused the blade to cool better near the root at low speeds, but the trend reversed at the leading edge at higher speeds (table II(c)). Definite conclusions as to the advantage or disadvantage of the dams cannot be drawn from the limited available data because the spanwise temperature distribution is so greatly affected by engine speed. It is known that on the basis of structure the dams are definitely detrimental.

4. The spanwise temperature distribution at the leading edge of blade 14 is affected by the coolant-flow rate at all speeds investigated. At high coolant-flow rates, the blade is cooler near the blade tip than near the root; but at low flow rates, the blade is cooler near the root (table II(d)).

5. Again from table II(d), the trailing-edge temperature distribution on blade 14 exhibits an effect of engine speed. The root portion of the blade is cooler than the tip portion at low speeds, but at higher speeds the trend is reversed so that the root portion is hotter. This trend is undesirable.

A conclusion that can be drawn from these spanwise-temperature-distribution studies is that the double-flow-type blades are probably slightly better with reference to the temperature distribution than the reverse-flow-type blade of reference 4; but because the cooling effectiveness of film-cooled blades is so greatly affected by coolant-flow rate and engine speed, the optimum spanwise temperature distribution can be approximated only over a very limited range of engine conditions.

Effect of engine speed on blade temperature. - The variation of blade temperature was determined over a range of engine speed for a coolant-flow ratio of 0.05. The blade-temperature variation is based on the effective gas temperature and coolant-temperature variations shown in figure 12, which is taken from reference 2.

Blade temperature is plotted against engine speed for thermocouples G, C, H, and J in figure 13. Figure 13(a) shows the variation of thermocouple G for blades 11, 12, and 14 compared with the 10-tube blade. Thermocouple Q for blade 14 is also shown, for it measured the leading-edge temperature on the opposite side of the leading-edge slot from G. In all of the blades except 14, thermocouple G shows an increasing trend with engine speed above 8000 rpm. This trend reflects an increase in gas temperature that occurs over this range. On blade 14, this trend is followed by thermocouple Q but thermocouple G shows a decreasing trend over this range, indicating that an increasing portion of the leading-edge film-cooling air is passing over the suction surface. This trend is probably caused by the change in angle of attack with engine speed, which affects the division of coolant flow over the blade. Blade 12 has the lowest leading-edge temperature over most of the speed range and all blades are cooler than the 10-tube blade.

In figure 13(b), which shows the trailing-edge thermocouple C, a similar trend is indicated; all the modified blades show substantial cooling over the entire range relative to the 10-tube blade. The variation of temperatures for midchord thermocouples H and J (figs. 13(c) and 13(d)) show that the modified blades have somewhat higher midchord temperatures than the 10-tube blade over most of the speed range.

Comparison of Correlated Cooling-Air Pressure Differences

The total and static pressures of the cooling air were measured at the turbine hub and the total pressure of the gas stream was measured in the tail pipe. The pressure required to force a given quantity of air through the blade cooling passages can be determined from these measurements if the pressure rise obtained by compressor action of the rotor is taken into account. The mathematical expression for this required pressure difference, corrected to standard conditions, is presented in reference 2 as

$$Y = \frac{\rho_{a,H}}{\rho_0}\left[p'_{a,H} - \left(p'_m - \frac{\eta\omega^2 r_T^2 \rho_{a,H}}{70.7}\right)\right] = f(w_a)$$

A value of $\eta = 0.27$ was found to correlate data for this turbine-rotor configuration and to give a curve that could be drawn through zero pressure difference at zero cooling-air flow. Figures 14(a), (b), and (c) show the pressure-difference correlations for blades 11, 12, and 14, respectively. Good correlation was obtained for the copper-clad blade (blade 11), but considerably more scatter was obtained for the film-cooled blades. Blade 11 had the lowest pressure drop of the three blades tested; the pressure drop was 43 inches of mercury at a coolant flow of 0.09. Blade 12 had a pressure drop of about 70 inches of mercury, and blade 14 had a pressure drop of about 77 inches of mercury at a coolant flow of 0.09 pound per second. The trend of scatter usually observed was followed by blade 12 with decreasing pressure drop with increasing engine speed. Blade 14 shows an unusual increase in pressure drop at engine speeds of 9000 and 10,000 rpm. This increase is believed to be caused by movement of the stagnation point closer to the single leading-edge slot, creating a higher discharge pressure.

The static-pressure drop from the rotor hub to the blade root was determined from measurements taken on a nonrotating wheel (reference 3). This pressure drop can be subtracted from the parameter Y to obtain the pressure drop through the blade itself. The corrected parameter, called Y_1, is plotted in figure 15 for blades 11, 12, and 14, and blade 8 of reference 4. Blade 11 has the lowest pressure drop. Blades 12 and 14 have approximately the same pressure drop and are substantially less than blade 8, which was a reverse-flow blade. This figure shows that the objective of the double-flow blade in reducing the pressure loss was achieved to a substantial degree.

The most desirable blade configuration would have a pressure drop that is as low as possible while achieving maximum cooling effectiveness. The blades can be compared on this basis in a plot like figure 16, where the cooling effectiveness φ for the trailing-edge thermocouple C is plotted against both cooling-air flow w_a and pressure-drop parameter Y_1. From this plot, the temperature-difference ratio and the blade pressure drop can be determined for a given coolant flow. For example, at high coolant flows, blade 8 has a higher trailing-edge cooling effectiveness than blade 11 but has a much higher pressure drop (fig. 16(a)) so that a choice between these two blade types would depend upon whether a higher coolant flow or a higher pressure drop could be tolerated for a given cooling effectiveness. For instance, at a coolant flow of 0.066 pound per second, blade 8 has a trailing-edge effectiveness φ_C of 0.430 and a pressure-drop parameter of about 68 inches of mercury. Blade 11 has about the same cooling effectiveness at an extrapolated coolant flow of about 0.092 pound per second per blade with a pressure drop of 27.5 inches of mercury. Blade 14 has the highest trailing-edge effectiveness for a given value of coolant flow and also the highest effectiveness for a given pressure-drop parameter.

The same type of plot is shown for the leading-edge cooling effectiveness in figure 16(b) for blades 11, 12, and 8. Blade 14 was not included in the leading-edge comparison because of the uneven flow distribution over the leading edge. The film-cooled blades 8 and 12 show the highest leading-edge cooling effectiveness at high flows but drop off much more rapidly as coolant flow is decreased than does the copper-clad blade (blade 11). This trend is reflected in the plot of φ_G against Y_1, where the film-cooled blades 8 and 12 show a larger pressure drop for a given leading-edge cooling effectiveness than blade 11, with the largest difference occurring at the lower flow rates. For a leading-edge cooling effectiveness of 0.300, blade 11 has a pressure drop of about 6 inches of mercury, blade 12 has a pressure drop of 20 inches of mercury, and blade 8 has a pressure drop of 29 inches of mercury.

The type of plot illustrated by figure 16 would be useful to designers of air-cooled engines because two important limitations in cooled-engine design are the amount of cooling air that can be supplied and the available cooling-air-supply pressure. The amount of cooling air is limited by the engine performance loss that can be tolerated, and the pressure available will be limited, in many cases, by the compressor-discharge pressure. A more complete discussion of the problems introduced by air-cooling a turbojet engine is given in reference 6.

PREDICTED ALLOWABLE TURBINE-INLET TEMPERATURES

The allowable sea-level turbine-inlet temperatures for the various blades were obtained by extrapolating the blade-temperature data to rated operating conditions. An allowable spanwise temperature curve for a nonstrategic alloy, Timken alloy 17-22A [S], was obtained from the stress-rupture characteristics of the material and the radial stress calculated from the centrifugal force on the blade. Then the allowable turbine-inlet temperature that gave blade temperatures not exceeding the allowable blade temperature at any point along the span was selected. The blade temperatures for the operating condition of 40,000-foot altitude were calculated from the cooling effectiveness data obtained at an engine air flow corresponding to the standard engine air flow for 40,000-foot altitude. This procedure is discussed in greater detail in reference 4.

The values of turbine-inlet temperature obtained in this way for the four blades investigated are given in table III. The design blade life is 1000 hours, but because only radial stresses due to centrifugal loading were taken into account, extensive endurance testing will be required for final evaluation of the service life of these configurations. The fact that the blades reported herein had fairly uniform chordwise temperature profiles makes the calculations more valid because the assumption of uniform strength over the cross section is more nearly approached than in blades that have high temperature gradients. In addition, a uniform temperature profile alleviated the thermal stresses in the blade, but the effects of vibratory stresses, which may be detrimental to the film-cooled blades, were neglected. Film-cooled blades are also more sensitive to coolant-flow ratio and pressure distribution around the blade than convection-cooled blades; therefore the predicted allowable turbine-inlet temperatures for this type of blade are probably less reliable than for the convection-cooled blade because of the need for predicting cooling characteristics for flow conditions that may not be the same as those of the investigation.

At sea level, the allowable turbine-inlet temperatures were predicted for two coolant temperatures: 510° F, which would be compressor-discharge temperature based on compressor-temperature-ratio curves from reference 1 plus an allowance of 100° temperature rise in the turbine wheel; and 200° F, which would be for the case when a heat exchanger was installed between the compressor discharge and the duct leading to the turbine blades. At an altitude of 40,000 feet, the cooling-air temperature was taken as 440° F, which was based on a flight Mach number of 0.8 and compressor-discharge temperature plus an allowance of 100° F.

The results indicate that when the midchord temperatures are used as the basis for comparison, all blades investigated could be made of nonstrategic material and operated at turbine-inlet temperatures of 1500° F or higher. Because of the higher trailing-edge temperatures, the allowable turbine-inlet temperatures based on trailing-edge temperature were correspondingly lower than those based on midchord temperature, but they probably would not limit the operating gas temperatures to less than 1500° F.

The allowable turbine-inlet-temperature calculations for the copper-clad blade were made for the case where the steel-shell dimensions were the same as those at the blades for which stresses have previously been calculated; but in addition, the inner surface of the blade shell was coated with copper to a thickness of 0.020 inch. The calculations were probably somewhat conservative because it was assumed that the copper coating as well as the copper tubes carried no load and were entirely supported by the steel shell.

SUMMARY OF RESULTS

The results of an experimental investigation of several air-cooled turbine blades with special modifications for cooling the leading and trailing edges of the blades are as follows:

1. A high-conductivity coating on the inside of the blade shell was the most effective method for reducing the temperature gradients in the cooled blades.

2. The use of a double-flow cooling-air path improved the cooling-air pressure loss relative to the original reverse-flow blade.

3. The use of a single row of larger leading-edge slots in place of a three-row arrangement apparently resulted in equally effective leading-edge cooling and provided a more structurally rigid leading-edge section, but one side of the blade was considerably cooler than the other side.

4. The leading-edge blade modifications in order of increasing cooling effectiveness for a coolant-flow ratio of 0.0534 were: (a) copper-clad leading edge, (b) three rows of 0.010-inch radial slots, and (c) a single row of 0.020-inch radial slots. All blades of this investigation had a sharp (0.05-in.) leading-edge radius.

5. The trailing-edge modifications investigated in order of increasing cooling effectiveness at a coolant-flow ratio of 0.0534 were: (a) copper-clad, and (b) radial slots.

6. At an engine speed of 10,000 rpm, an effective gas temperature of 1070° F, a coolant- to gas-flow ratio of 0.0534, and a cooling-air inlet temperature at the blade root of 130° F, the temperatures of the leading edges of blades 11, 12, and 14 were 850°, 780°, and 720° F, respectively, and the average midchord temperatures were about 660°, 635°, and 660° F, respectively. The trailing-edge temperatures of blades 11, 12, and 14 were 720°, 670°, and 610° F, respectively.

7. The rate of decrease in cooling effectiveness as coolant flow rate was decreased was greater for the film-cooled blades than for the copper-clad blade, particularly at low coolant-flow rates.

8. The cooling-air pressure loss for a given coolant-flow rate was lowest for blade 11.

9. All blades of this investigation would probably be capable of operation at 1500° F turbine-inlet temperature at a coolant-flow ratio of 0.05.

Lewis Flight Propulsion Laboratory,
National Advisory Committee for Aeronautics,
Cleveland, Ohio.

REFERENCES

1. Ellerbrock, Herman H., Jr., and Stepka, Francis S.: Experimental Investigation of Air-Cooled Turbine Blades in Turbojet Engine. I - Rotor Blades with 10 Tubes in Cooling-Air Passages. NACA RM E50I04, 1950.

2. Hickel, Robert O., and Ellerbrock, Herman H., Jr.: Experimental Investigation of Air-Cooled Turbine Blades in Turbojet Engine. II - Rotor Blades With 15 Fins in Cooling-Air Passages. NACA RM E50I14, 1950.

3. Hickel, Robert O., and Smith, Gordon T.: Experimental Investigation of Air-Cooled Turbine Blades in Turbojet Engine. III - Rotor Blades With 34 Steel Tubes in Cooling-Air Passages. NACA RM E50J06, 1950.

4. Ellerbrock, Herman H., Jr., Zalabak, Charles F., and Smith, Gordon T.: Experimental Investigation of Air-Cooled Turbine Blades in Turbojet Engine. IV - Effects of Special Leading- and Trailing-Edge Modifications on Blade Temperature. NACA RM E51A19, 1951.

5. Smith, Gordon T., and Hickel, Robert O.: Experimental Investigation of Air-Cooled Turbine Blades in Turbojet Engine. V - Rotor Blades With Split Trailing Edges. NACA RM E51A22, 1951.

6. Schramm, Wilson B., Nachtigall, Alfred J., and Arne, Vernon L.: Preliminary Analysis of Effects of Air Cooling Turbine Blades on Turbojet-Engine Performance. NACA RM E50E22, 1950.

TABLE I - SUMMARY OF GEOMETRY FACTORS AND MODIFICATIONS FOR BLADES INVESTIGATED

Item	Blade			
	11	12	13	14
Total free-flow area of internal cooling-air passages, (sq in.)	0.20	Leading- and trailing-edge passages, 0.08; tubed passages, 0.11	Leading- and trailing-edge passages, 0.08; tubed passages, 0.11	Leading- and trailing-edge passages, 0.08; tubed passages, 0.11
Total surface area of internal cooling-air passages, (sq in.)	29.6	Leading- and trailing-edge passages, 8.0; tubed passages, 14.8	Leading- and trailing-edge passages, 8.0; tubed passages, 14.8	Leading- and trailing-edge passages, 8.0; tubed passages, 14.8
Total perimeter of internal cooling-air passages, (in.)	7.4	Leading- and trailing-edge passages, 2.0; tubed passages, 3.7	Leading- and trailing-edge passages, 2.0; tubed passages, 3.7	Leading- and trailing-edge passages, 2.0; tubed passages, 3.7
Hydraulic diameter of internal cooling-air passages, (in.)	0.108	Average of leading- and trailing-edge passages, 0.16; tubed passages, 0.12	Average of leading- and trailing-edge passages, 0.16; tubed passages, 0.12	Average of leading- and trailing-edge passages, 0.16; tubed passages, 0.12
Leading-edge modifications	[a]0.020-inch copper-clad coating on inside surface	[b]Radial leading-edge slots with dam across leading-edge passage at midspan; three rows of 0.010-inch slots; passage open to coolant at blade root	Same as blade 12 with dam removed	[c]Single slot 0.020 inch wide; passage open to coolant at blade root; no dam in passage
Trailing-edge modifications	0.020-inch copper-clad coating on inside surface	Radial slot 0.025 inch wide; dam across trailing-edge passage at midspan; passage open to coolant at blade root	Same as blade 12 with dam removed	Same as blade 12 with dam removed

[a]See figure 1.
[b]See figure 2.
[c]See figure 3.

TABLE II - SUMMARY OF ENGINE OPERATING CONDITIONS AND TEMPERATURE-DIFFERENCE RATIOS

(a) Blade 11.

Series	Engine speed N (rpm)	Effective gas temperature $T_{g,e}$ (°F)	Average conditions at compressor inlet: Total pressure $p'_{A,c,i}$ (in. Hg)	Average conditions at compressor inlet: Total temperature $T'_{A,c,i}$ (°F)	Cooling-air flow per blade w_a (lb/sec)	Coolant flow per blade: Combustion-gas flow per blade	Temperature-difference ratio φ: Thermocouple G	J	I	H
1	4,000	954	28.88	66	0.090	0.229	0.581	0.673	0.623	0.652
	4,000				.071	.179	.553	.638	.587	.617
	4,000				.050	.127	.511	.590	.536	.569
	4,000				.040	.102	.478	.559	.506	.540
	4,000				.030	.077	.454	.521	.474	.501
	4,000				.025	.062	.417	.488	.446	.475
	4,000				.020	.050	.393	.466	.425	.454
	4,000				.015	.038	.369	.444	.406	.430
	4,000				.010	.026	.330	.407	.370	.394
	4,000				.005	.013	.284	.353	.329	.345
2	6,000	910	28.88	66	0.090	0.144	0.507	0.610	0.540	0.574
	6,000				.071	.114	.476	.574	.505	.540
	6,000				.050	.080	.432	.528	.463	.495
	6,000				.040	.065	.404	.493	.436	.467
	6,000				.030	.049	.374	.465	.412	.440
	6,000				.025	.040	.359	.453	.402	.428
	6,000				.020	.032	.333	.427	.382	.405
	6,000				.015	.024	.309	.403	.362	.382
	6,000				.010	.016	.274	.371	.340	.347
5	10,000	1069	29.48	68	0.089	0.082	0.384	0.514	0.430	0.464
	10,000				.070	.064	.349	.478	.404	.433
	10,000				.059	.054	.328	.457	.388	.414
	10,000				.049	.045	.306	.436	.375	.397
	10,000				.040	.037	.286	.421	.363	.382
	10,000				.030	.028	.270	.384	.348	.361
							A	C	D	P
1	4,000	951	28.90	67	0.090	0.228	0.536	0.616	0.633	0.491
	4,000				.070	.178	.509	.588	.610	.471
	4,000				.049	.125	.469	.543	.572	.436
	4,000				.040	.102	.453	.515	.548	.408
	4,000				.030	.077	.440	.480	.522	.379
	4,000				.024	.062	.423	.459	.501	.359
	4,000				.020	.050	.409	.443	.493	.342
	4,000				.015	.038	.383	.418	.471	.321
	4,000				.010	.026	.346	.392	.450	.291
	4,000				.005	.013	.283	.344	.419	.293
2	6,000	918	28.90	67	0.090	0.144	0.480	0.546	0.552	0.424
	6,000				.070	.113	.466	.517	.528	.402
	6,000				.049	.079	.461	.477	.488	.363
	6,000				.040	.065	.452	.455	.470	.344
	6,000				.030	.049	.434	.436	.459	.318
	6,000				.025	.040	.412	.415	.443	.300
	6,000				.020	.032	.391	.399	.431	.279
	6,000				.013	.021	.349	.372	.412	.253
	6,000				.010	.016	.323	.355	.399	.234
5	10,000	1064	29.51	83	0.089	0.082	0.499	0.424	0.502	0.304
	10,000				.075	.069	.491	.404	.492	.283
	10,000				.070	.064	.482	.404	.493	.243
	10,000				.057	.052	.461	.383	.469	.226
	10,000				.049	.045	.444	.369	.450	.210
	10,000				.040	.037	.422	.355	.442	.195
	10,000				.030	.027	.397	.340	.429	.175

NACA

TABLE II - SUMMARY OF ENGINE OPERATING CONDITIONS AND TEMPERATURE-DIFFERENCE RATIOS - Continued

(b) Blade 12.

Series	Engine speed N (rpm)	Effective gas temperature $T_{g,e}$ (°F)	Average conditions at compressor inlet: Total pressure $p'_{A,c,i}$ (in. Hg)	Average conditions at compressor inlet: Total temperature $T'_{A,c,i}$ (°F)	Cooling-air flow per blade w_a (lb/sec)	Coolant flow per blade: Combustion-gas flow per blade	Temperature-difference ratio φ: Thermocouple G	H	V	J
	4,000				0.098	0.272	0.657	0.699	0.557	0.682
	4,000				.089	.247	.643	.687	.548	.678
	4,000				.070	.194	.629	.662	.524	.672
	4,000				.049	.137	.629	.629	.493	.642
6	4,000	1035	29.05	82	.040	.112	.622	.606	.465	.620
	4,000				.030	.083	.610	.569	.417	.587
	4,000				.024	.067	.585	.539	.380	.557
	4,000				.020	.055	.543	.510	.341	.525
	4,000				.015	.041	.432	.467	.284	.475
	4,000				.010	.028	.240	.408	.226	.409
	6,000				0.089	0.155	0.665	0.659	0.532	0.678
	6,000				.069	.120	.663	.639	.502	.657
	6,000				.060	.104	.661	.614	.481	.639
	6,000				.050	.087	.647	.583	.451	.614
7	6,000	978	29.05	88	.040	.070	.612	.547	.409	.587
	6,000				.030	.052	.526	.505	.343	.533
	6,000				.024	.042	.415	.477	.304	.499
	6,000				.020	.034	.235	.438	.256	.441
	6,000				.015	.025	.140	.375	.219	.380
	6,000				.010	.018	.066	.313	.175	.306
	10,000				0.100	0.090	0.626	0.586	0.457	0.598
	10,000				.091	.082	.593	.567	.429	.569
10	10,000	1047	29.48	78	.071	.064	.467	.526	.358	.501
	10,000				.061	.055	.358	.496	.311	.444
	10,000				.050	.045	.185	.455	.278	.374
							A	C	T	U
	4,000				0.090	0.249	0.646	0.578	0.770	0.834
	4,000				.071	.195	.616	.558	.743	.812
	4,000				.060	.166	.597	.549	.729	.787
	4,000				.051	.140	.575	.544	.705	.766
6	4,000	1034	29.36	85	.040	.111	.549	.539	.674	.747
	4,000				.036	.099	.509	.530	.655	.732
	4,000				----	----	.500	.511	.625	.713
	4,000				.024	.067	.453	.479	.585	.680
	4,000				.020	.054	.407	.436	.538	.623
	4,000				.015	.041	.343	.344	.498	.562
	4,000				.010	.028	.281	.205	.461	.479
	6,000				0.091	0.156	0.624	0.598	0.731	0.843
	6,000				.071	.122	.598	.590	.705	.791
	6,000				.061	.105	.578	.583	.683	.772
	6,000				.050	.086	.547	.562	.649	.751
7	6,000	1000	29.36	91	.041	.070	.498	.523	.598	.702
	6,000				.031	.053	.426	----	.531	.621
	6,000				.024	.042	.390	----	.510	.577
	6,000				.020	.034	.348	----	.485	.510
	6,000				.015	.026	.314	.187	.472	.440
	6,000				.010	.018	.263	.119	.447	.328
	8,000				0.090	0.111	0.611	0.699	0.618	0.826
	8,000				.071	.087	.561	.650	.583	.761
	8,000				.060	.074	.528	.614	.559	.733
10	8,000	986	29.40	102	.050	.062	.483	.567	.518	.695
	8,000				.040	.049	.434	.528	.452	.641
	8,000				.030	.037	.387	.493	.293	.513
	8,000				.024	.030	.362	.480	.230	.446
	8,000				.020	.025	.333	.469	.195	.373
	8,000				.015	.018	.293	.457	.133	.287

NACA

TABLE II - SUMMARY OF ENGINE OPERATING CONDITIONS AND TEMPERATURE-DIFFERENCE RATIOS - Continued

(c) Blade 13.

Series	Engine speed N (rpm)	Effective gas temperature $T_{g,e}$ (°F)	Average conditions at compressor inlet		Cooling-air flow per blade w_a (lb/sec)	Coolant flow per blade / Combustion-gas flow per blade	Temperature-difference ratio φ			
			Total pressure $p'_{A,c,i}$ (in. Hg)	Total temperature $T'_{A,c,i}$ (°F)			Thermocouple			
							A	C	T	U
11	4,000	1027	29.37	81	0.090	0.244	0.625	0.760	0.626	0.781
	4,000				.071	.193	.605	.733	.605	.751
	4,000				.061	.165	.594	.717	.594	.737
	4,000				.049	.133	.564	.696	.585	.727
	4,000				.041	.111	.533	.670	.578	.714
	4,000				.030	.081	.482	.620	.553	.688
	4,000				.025	.068	.448	.578	.528	.671
	4,000				.020	.054	.397	.532	.482	.608
	4,000				.015	.041	.336	.492	.403	.481
	4,000				.010	.027	.281	.463	.262	.400
12	6,000	967	29.37	87	0.090	0.152	(a)	0.730	0.645	0.777
	6,000				.071	.120		.708	.630	.745
	6,000				.050	.084		.644	.607	.698
	6,000				.041	.069		.591	.574	.672
	6,000				.030	.050		.526	.505	.549
	6,000				.025	.042		.505	.437	.475
	6,000				.020	.034		.486	.319	.414
	6,000				.015	.025		.471	.236	.358
	6,000				.010	.017		.447	.153	.299
15	10,000	1059	29.48	80	0.100	0.090	0.443	0.562	0.743	0.534
	10,000				.091	.082	.421	.530	.727	.499
	10,000				.071	.064	.376	.468	.689	.435
	10,000				.061	.055	.344	.437	.636	.385
	10,000				.051	.046	.315	.416	.524	.346

[a]Thermocouple inoperative.

TABLE II - SUMMARY OF ENGINE OPERATING CONDITIONS AND TEMPERATURE-DIFFERENCE RATIOS - Concluded

(d) Blade 14.

Series	Engine speed N (rpm)	Effective gas temperature $T_{g,e}$ (°F)	Average conditions at compressor inlet: Total pressure $p'_{A,c,i}$ (in. Hg)	Average conditions at compressor inlet: Total temperature $T'_{A,c,i}$ (°F)	Cooling-air flow per blade w_a (lb/sec)	Coolant flow per blade / Combustion-gas flow per blade	Temperature-difference ratio Φ: Thermocouple G	H	Q	J
16	4,000	1031	29.16	65	0.0995	0.265	0.588	0.071	0.573	0.672
	4,000				.0908	.242	.585	.685	.560	.661
	4,000				.0709	.189	.540	.643	.525	.629
	4,000				.0494	.132	.507	.594	.479	.585
	4,000				.0405	.108	.496	.564	.452	.565
	4,000				.0302	.081	.465	.518	.396	.521
	4,000				.0244	.065	.445	.491	.362	.497
	4,000				.0195	.052	.411	.454	.320	.460
	4,000				.0148	.040	.365	.406	.274	.408
	4,000				.0100	.027	.271	.337	.203	.334
17	6,000	973	29.16	65	0.0999	0.166	0.586	0.646	0.523	0.625
	6,000				.0906	.151	.575	.627	.510	.623
	6,000				.0713	.119	.554	.594	.484	.590
	6,000				.0496	.083	.526	.539	.433	.539
	6,000				.0408	.068	.500	.509	.394	.509
	6,000				.0304	.051	.440	.454	.312	.460
	6,000				.0246	.041	.398	.422	.268	.420
	6,000				.0198	.033	.336	.385	.229	.376
					.0149	.025	.145	.335	.102	.305
20	10,000	1028	29.16	67	0.100	0.090	0.714	0.466	0.420	0.582
	10,000				.091	.082	.719	.447	.416	.577
	10,000				.071	.064	.683	.423	.404	.521
	10,000				.061	.055	.650	.406	.374	.471
	10,000				.050	.045	.607	.381	.311	.433
	10,000				.042	.038	----	.342	.195	.385
							A	C	T	U
16	4,000	1036	29.14	67	0.0994	0.264	0.724	0.793	0.768	0.708
	4,000				.0904	.240	.714	.791	.752	.686
	4,000				.0710	.189	.676	.773	.688	.636
	4,000				.0500	.133	.600	.722	.599	.559
	4,000				.0480	.108	.552	.689	.533	.521
	4,000				.0301	.080	.480	.636	.432	.469
	4,000				.0246	.065	.443	.600	.379	.443
	4,000				.0197	.052	.395	.551	.314	.414
	4,000				.0149	.040	.328	.502	.222	.391
17	6,000	955	29.24	61	0.0908	0.149	0.693	0.739	0.704	0.650
	6,000				.0710	.117	.633	.707	.642	.596
	6,000				.0500	.082	.553	.655	.536	.532
	6,000				.0304	.050	.436	.538	.368	.459
	6,000				.0195	.032	.351	.480	.189	.333
20	10,000	1074	29.13	79	0.100	0.093	0.624	0.604	0.694	0.659
	10,000				.091	.084	.609	.589	.672	.639
	10,000				.071	.066	.563	.532	.616	.585
	10,000				.050	.046	.490	.459	.496	.524
					.041	.038	.450	.421	.372	.426

NACA

TABLE III - PREDICTED ALLOWABLE TURBINE-INLET TEMPERATURES FOR TIMKEN ALLOY 17-22A[S]

[Engine speed, 11,500 rpm; cooling-air-flow rate, 5 percent of combustion-gas-flow rate; standard sea-level, static compressor-inlet air; flight Mach number of 0.8 at 40,000 feet.]

Blade	Cooling-air inlet temperature $T_{a,e,h}$ (°F)	Allowable turbine-inlet temperature, °F			
		Based on trailing-edge temperatures		Based on midchord temperatures	
		Sea level	40,000 feet	Sea level	40,000 feet
11	510	1480		1520	
	200	1650		1720	
	440		1560		1620
12	510	1440		1660	
	200	1530		1900	
	440		1580		1860
[a]13	510	1460		---	
	200	1560		---	
	440		1710		---
14	510	1460		1640	
	200	1560		1860	
	440		1770		1750

[a]No midchord temperatures measured.

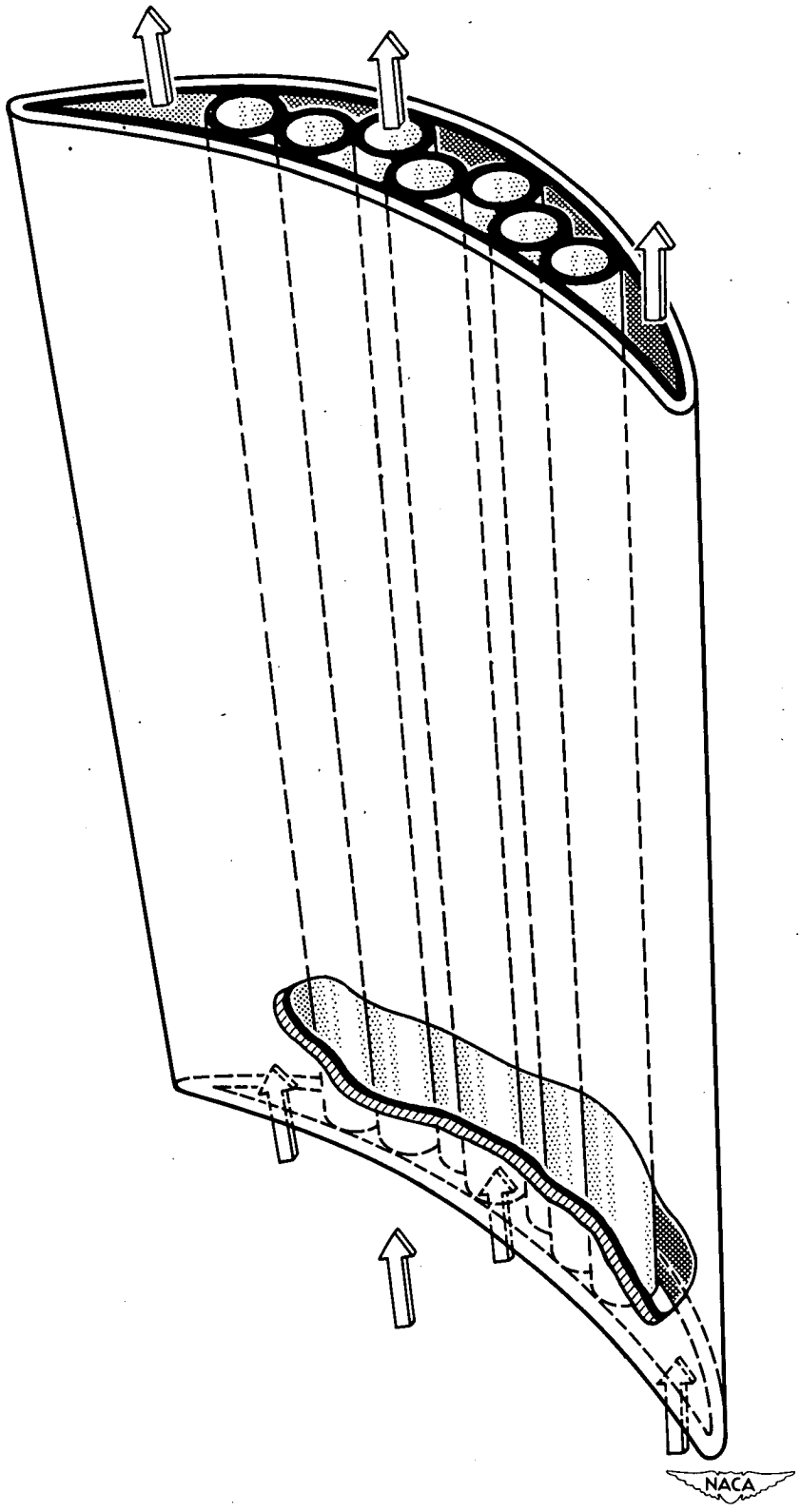

Figure 1. - Blade 11; copper-clad shell containing seven copper tubes.

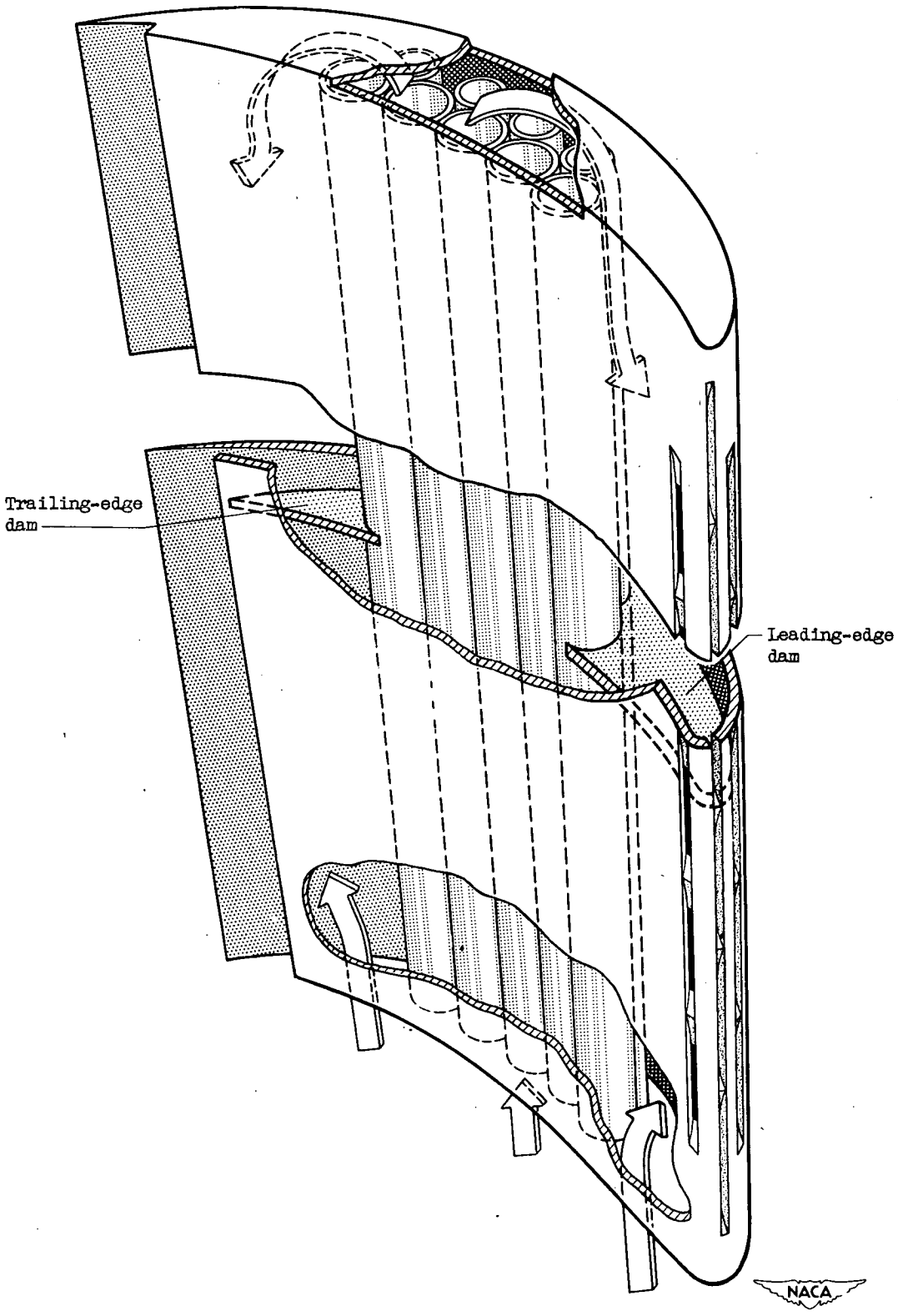

Figure 2. - Blade 12; double-flow blade with three rows of leading-edge slots.

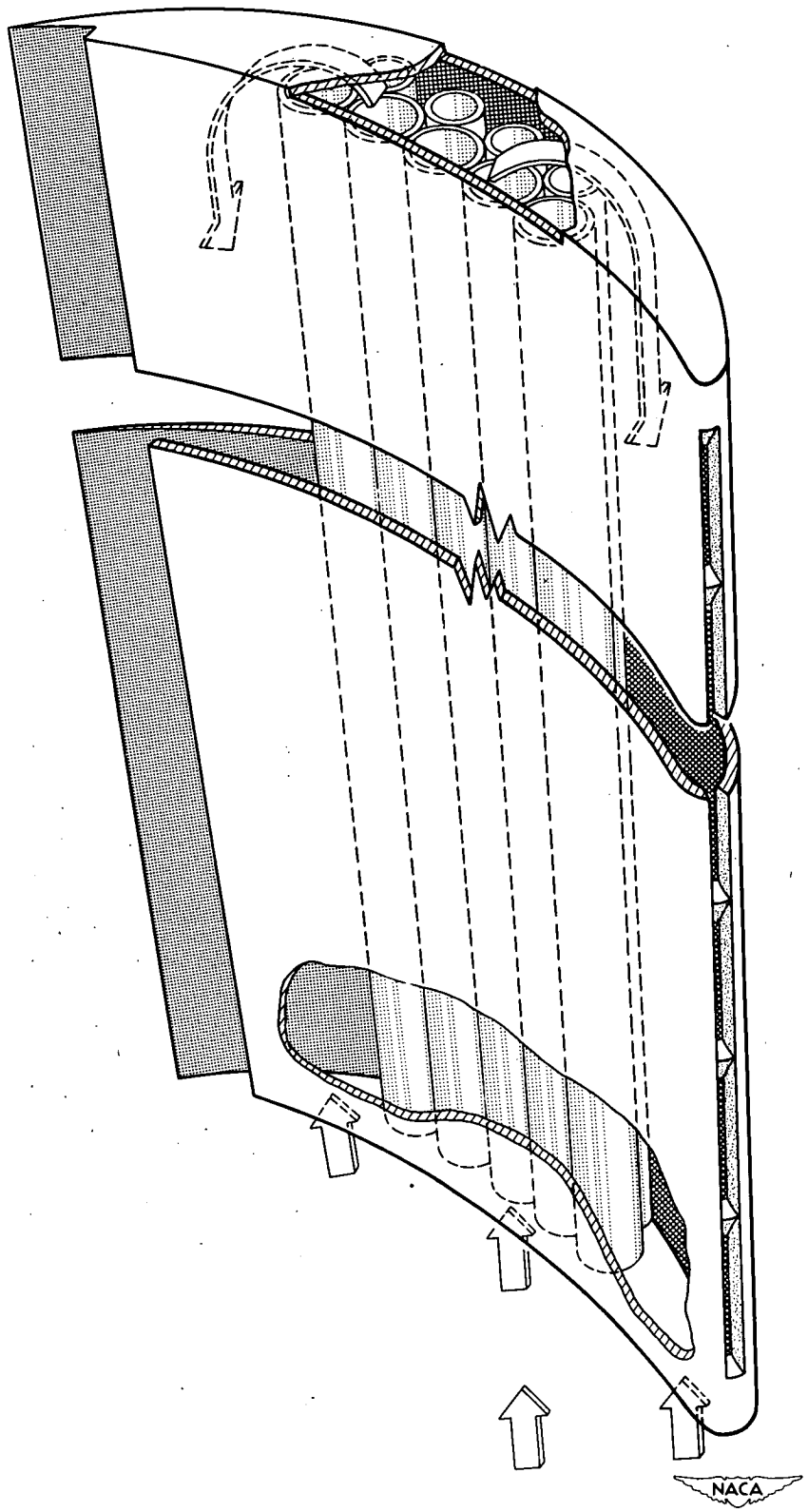

Figure 3. - Blade 14; double-flow blade with one row of leading-edge slots.

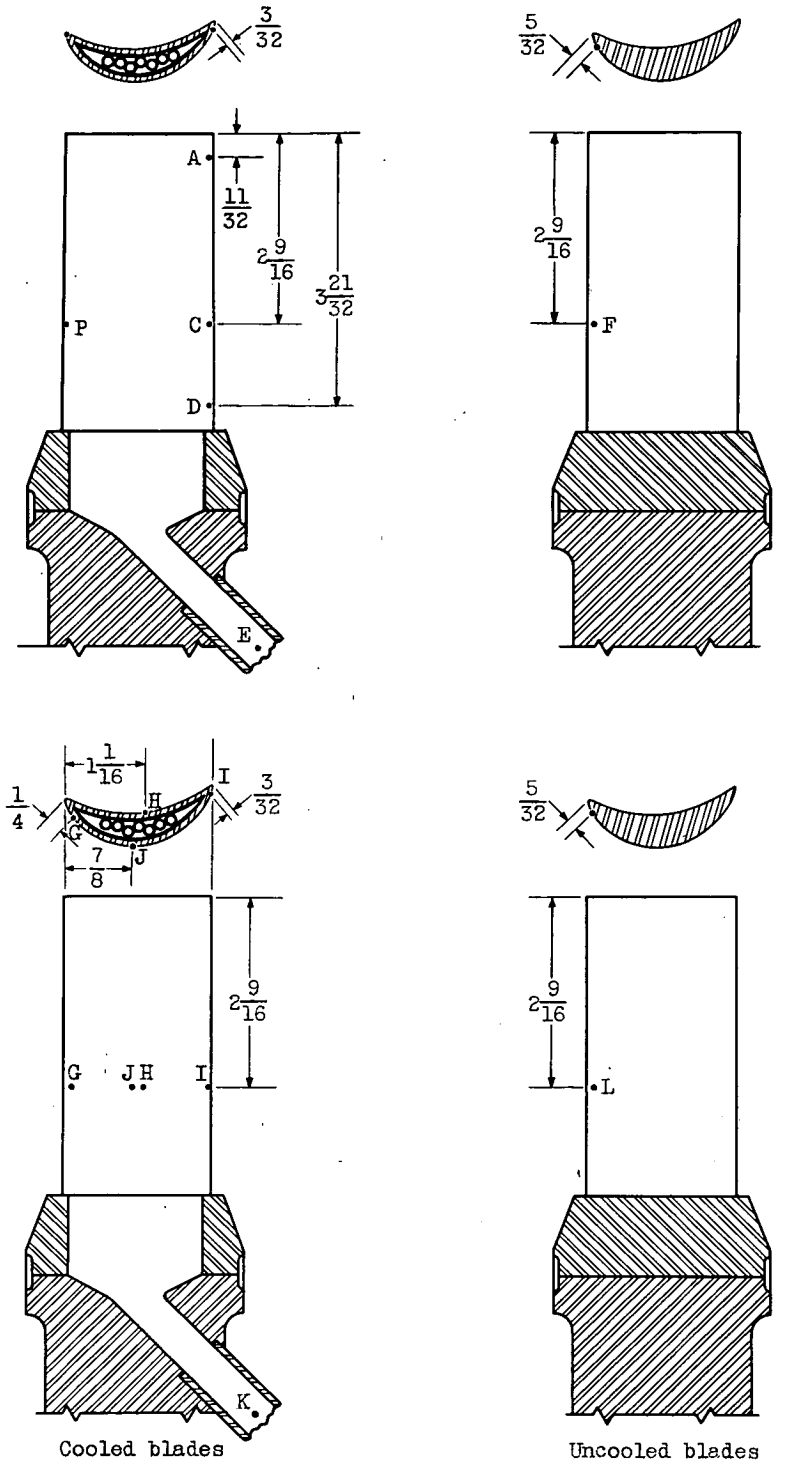

(a) Blade 11.

Figure 4. - Schematic diagram of thermocouple locations on cooled and uncooled blades investigated. (Dimensions in inches.)

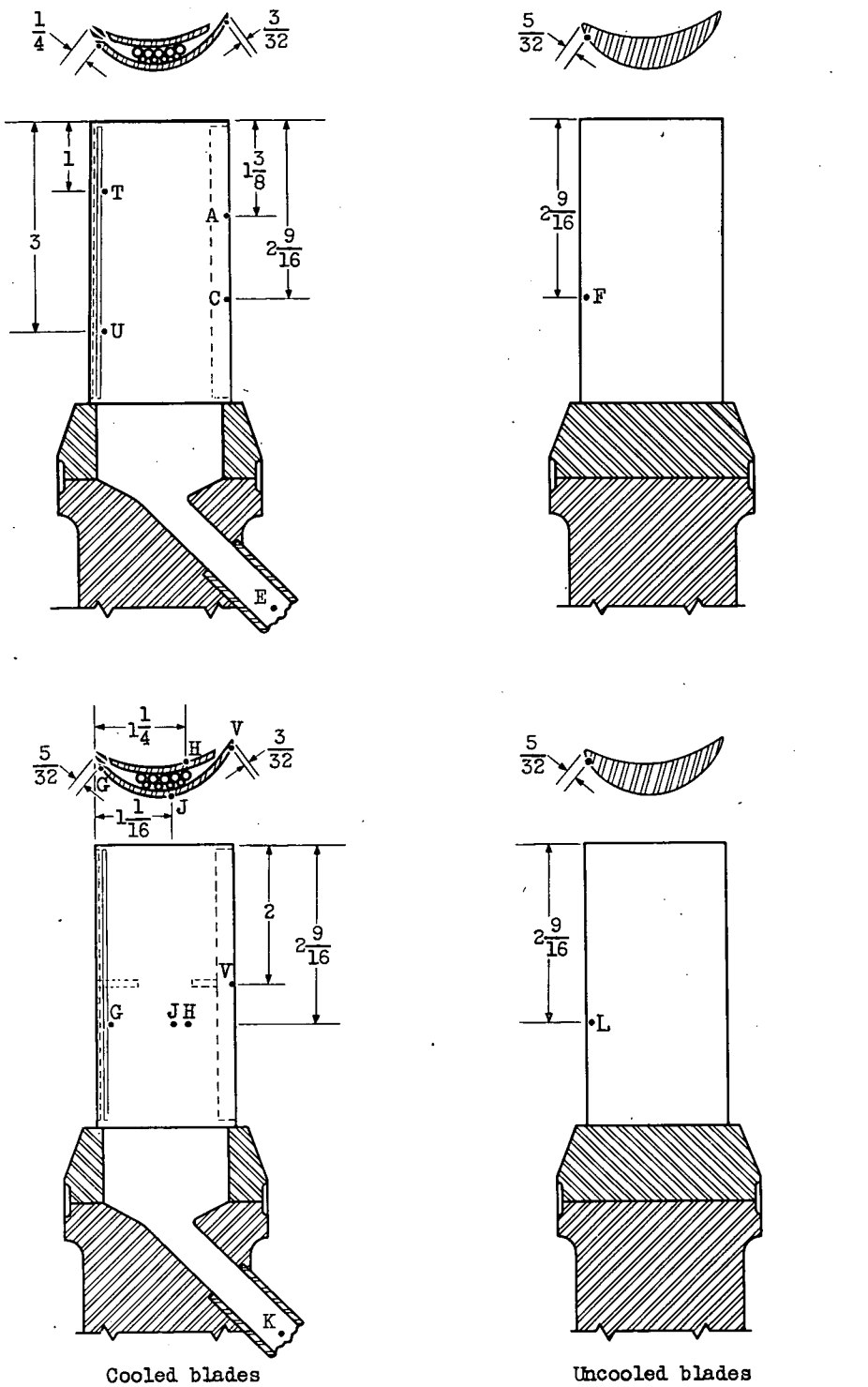

(b) Blades 12 and 13.

Figure 4. - Continued. Schematic diagram of thermocouple locations on cooled and uncooled blades investigated. (Dimensions in inches.)

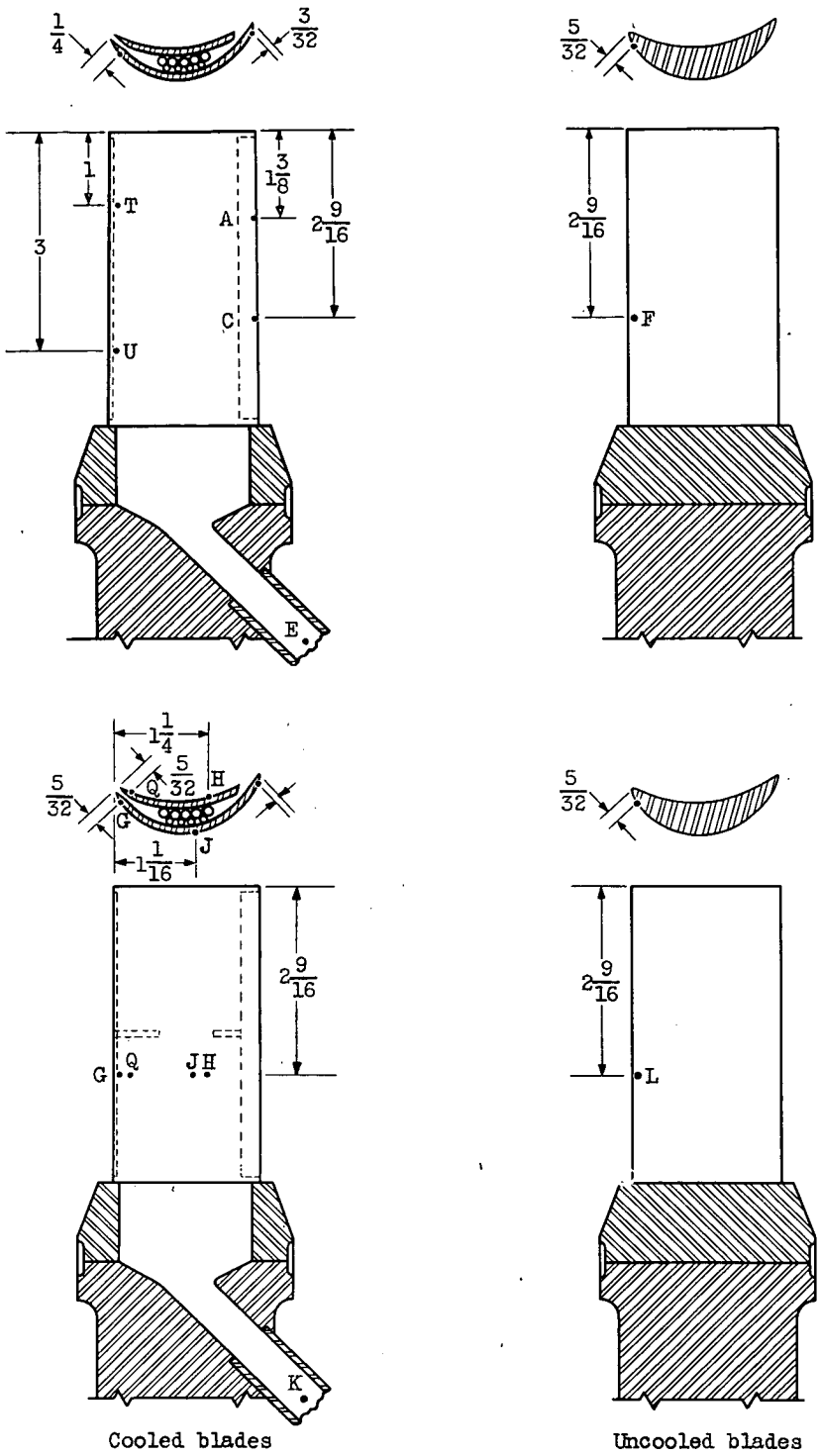

(c) Blade 14.

Figure 4 . - Concluded. Schematic diagram of thermocouple locations on cooled and uncooled blades investigated. (Dimensions in inches.)

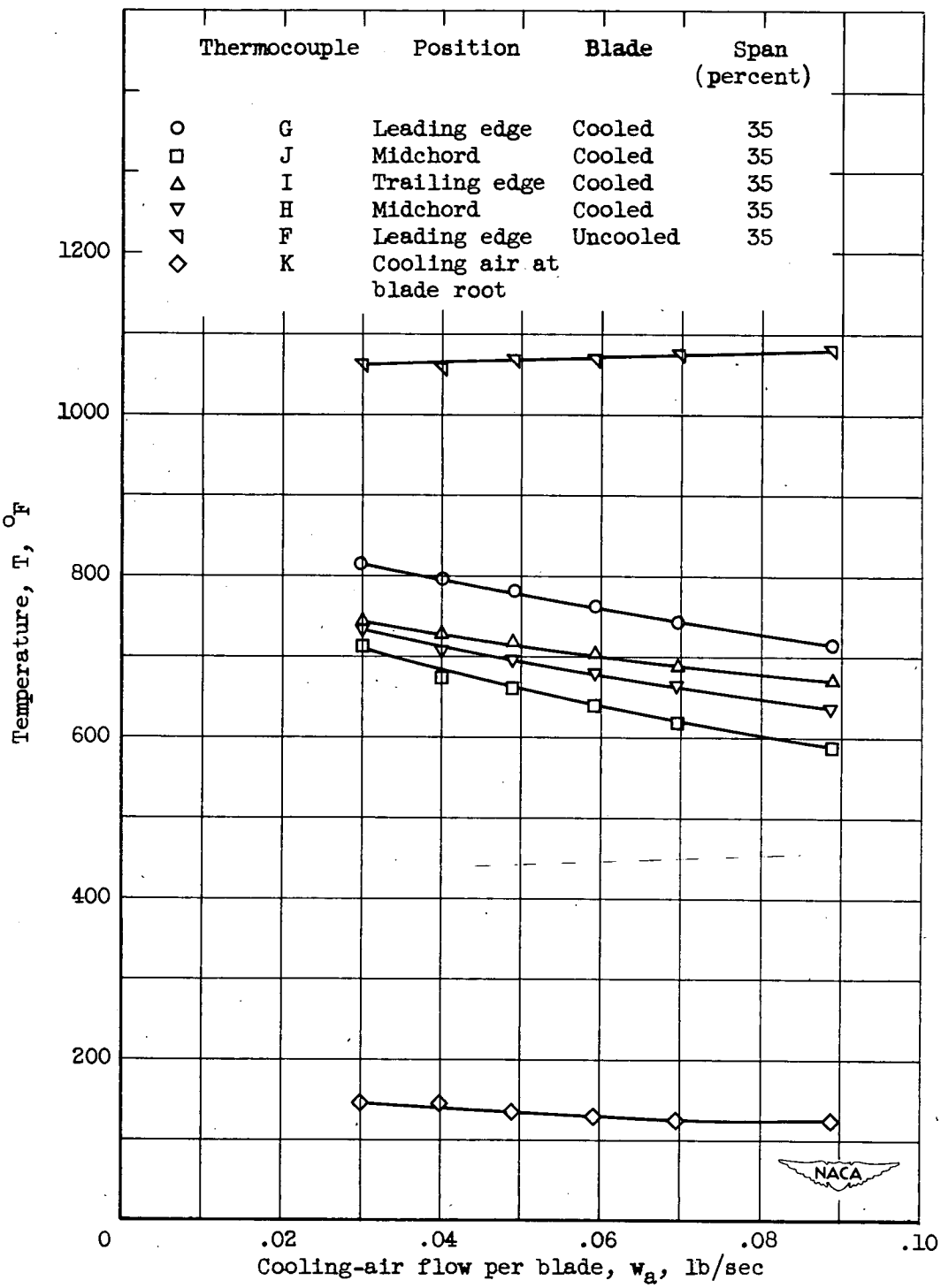

(a) Thermocouples G, J, I, H, K, and F.

Figure 5. - Effect of cooling-air-flow rate on blade and cooling-air temperatures for blade 11 at engine speed of 10,000 rpm.

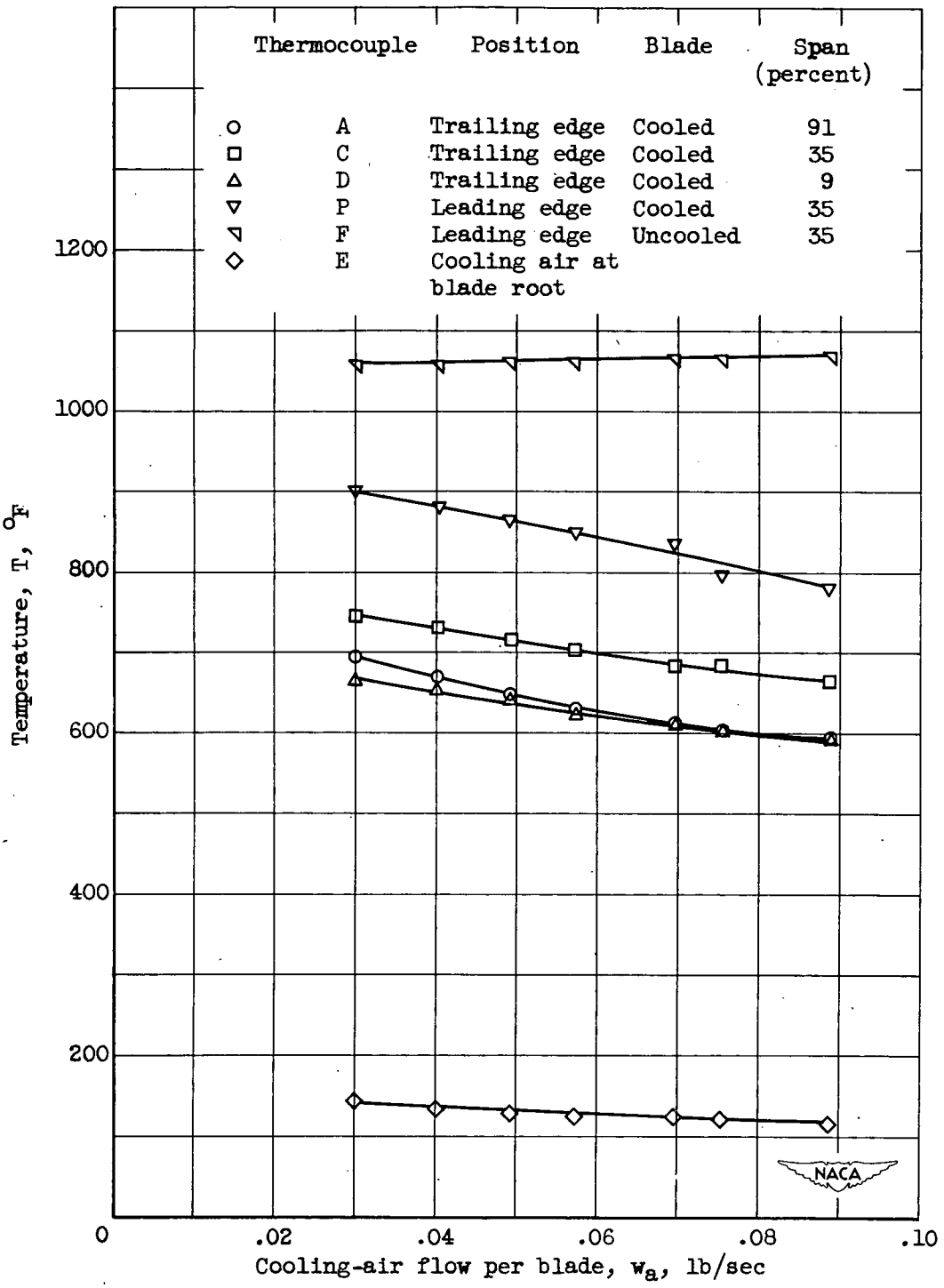

(b) Thermocouples A, C, D, P, E, and F.

Figure 5. - Concluded. Effect of cooling-air-flow rate on blade and cooling-air temperatures for blade 11 at engine speed of 10,000 rpm.

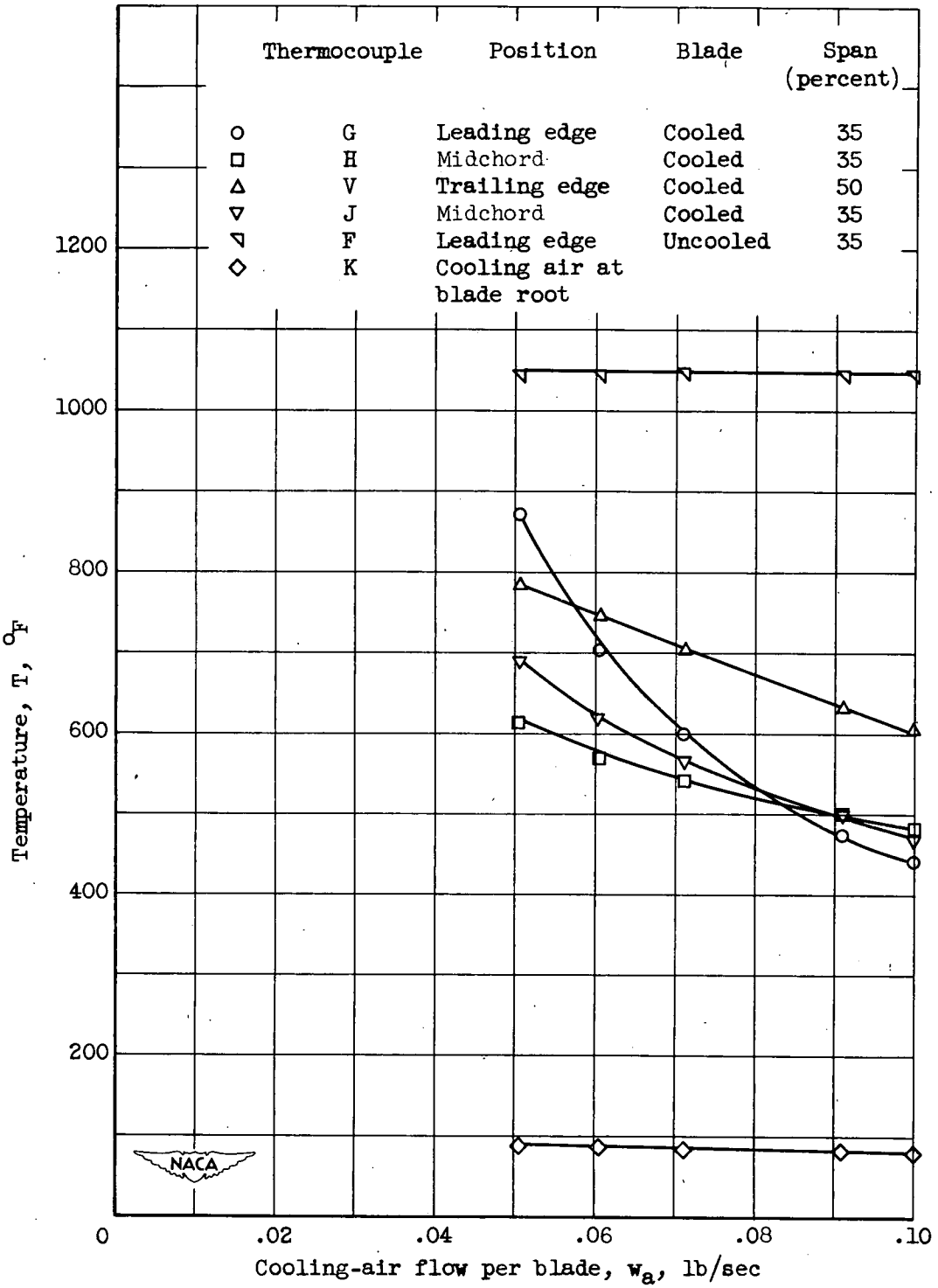

(a) Thermocouples G, H, V, J, K, and F. Engine speed, 10,000 rpm.

Figure 6. - Effect of cooling-air-flow rate on blade and cooling-air temperatures for blade 12.

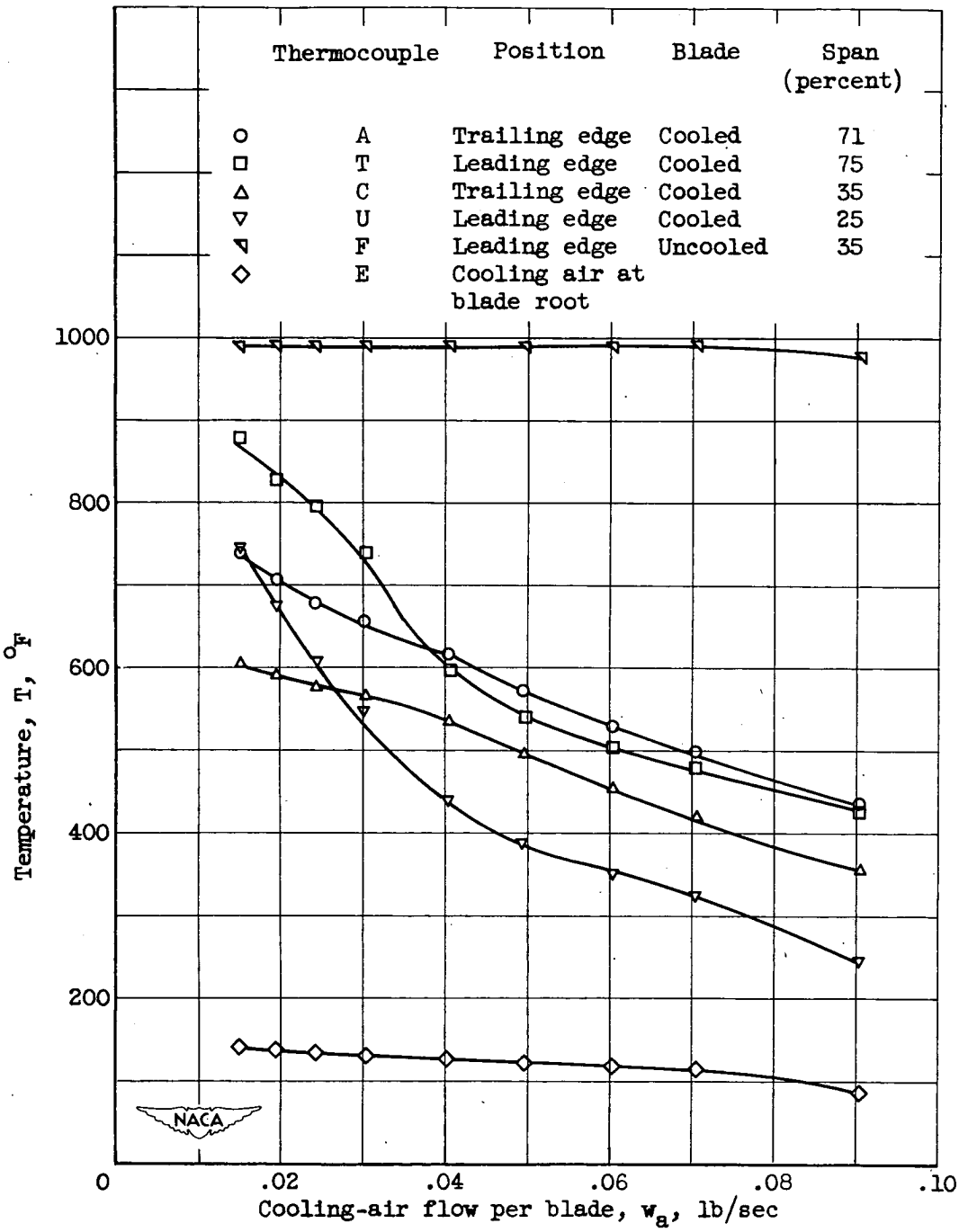

(b) Thermocouples A, T, C, U, E, and F. Engine speed, 8000 rpm.

Figure 6. - Concluded. Effect of cooling-air-flow rate on blade and cooling-air temperatures for blade 12.

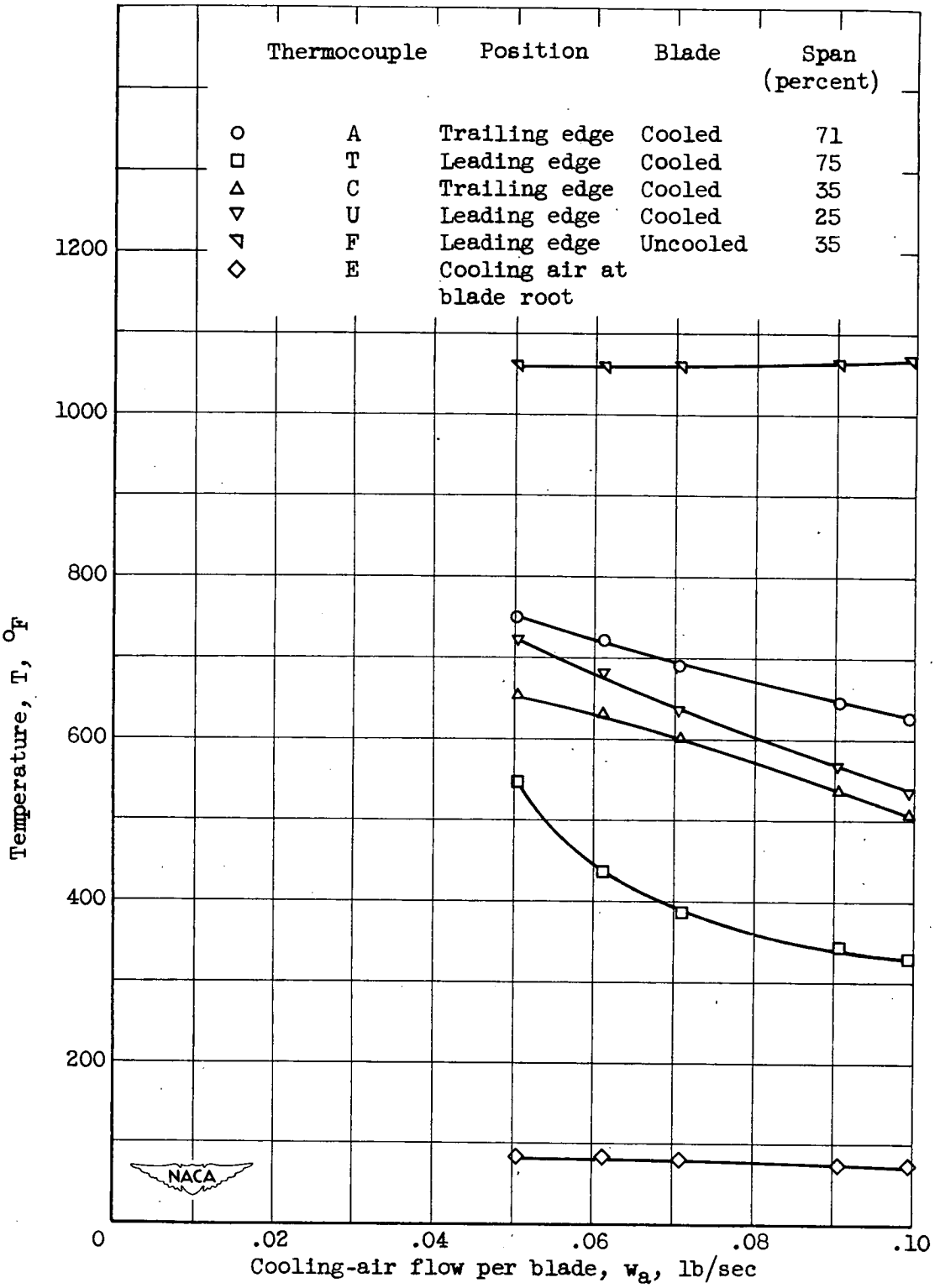

Figure 7. - Effect of cooling-air-flow rate on blade and cooling-air temperatures for blade 13 at engine speed of 10,000 rpm.

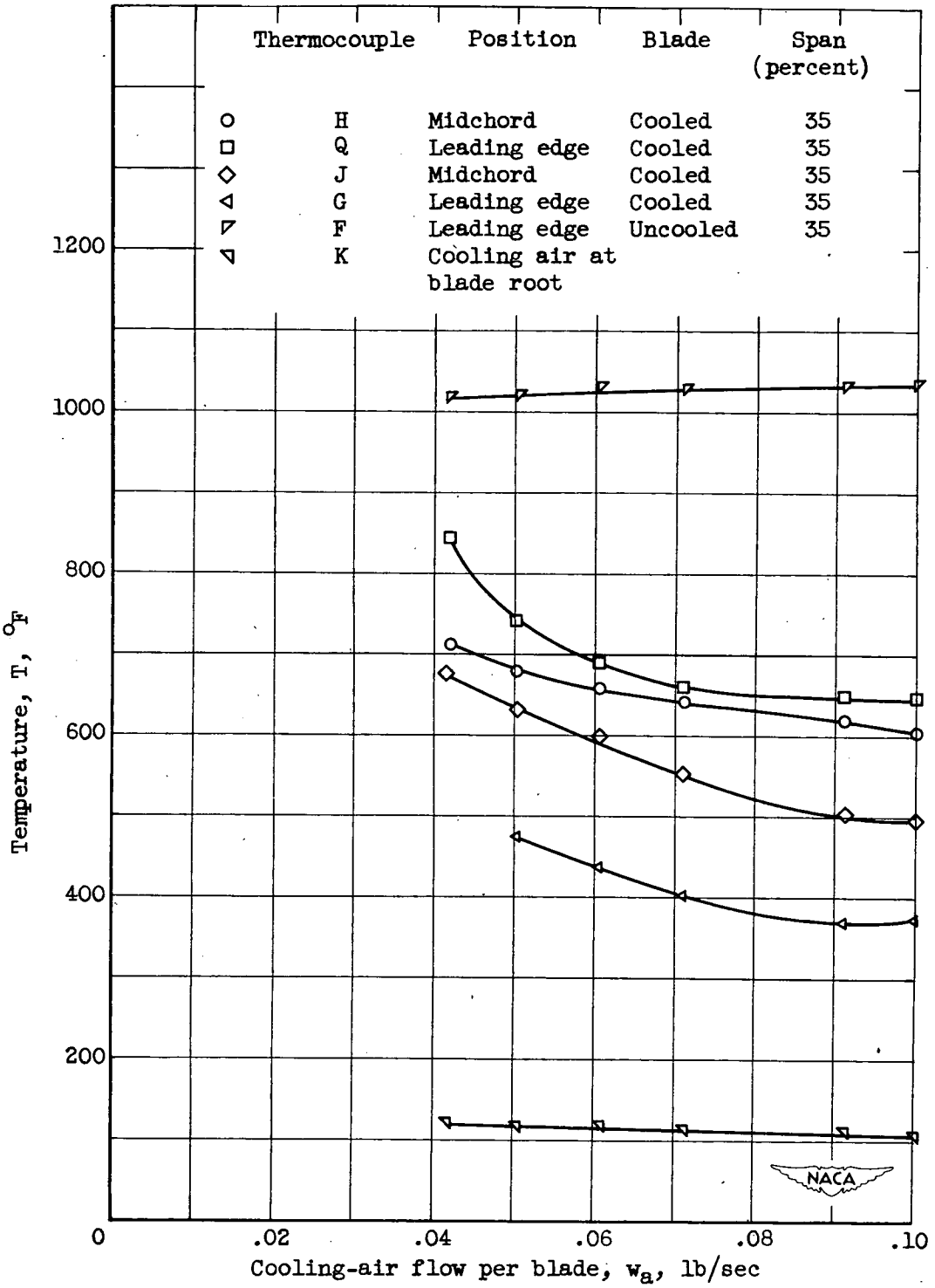

(a) Thermocouples H, Q, J, G, K, and F.

Figure 8. - Effect of cooling-air-flow rate on blade and cooling-air temperatures for blade 14 at 10,000 rpm.

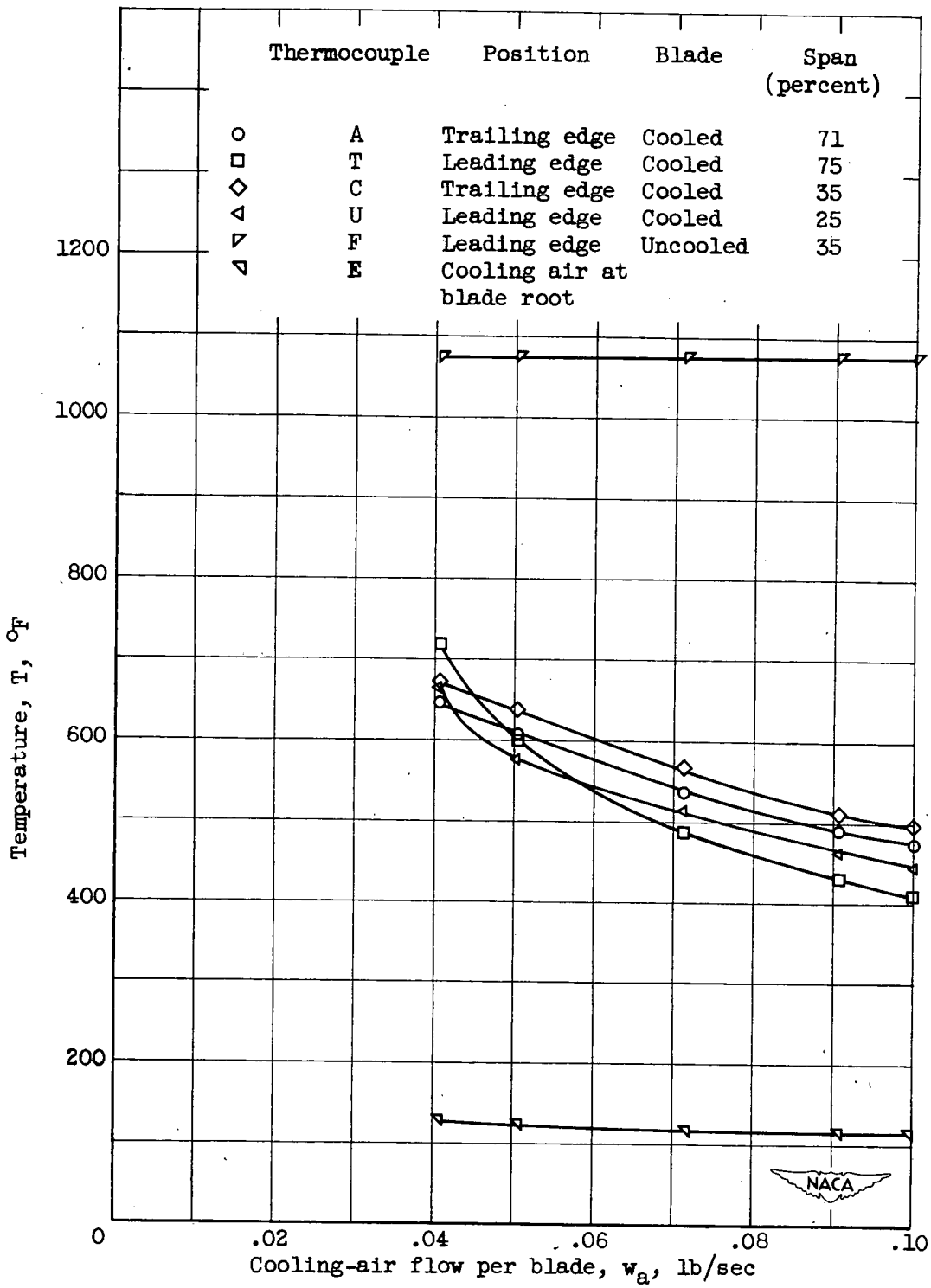

(b) Thermocouples A, T, C, U, E, and F.

Figure 8. - Concluded. Effect of cooling-air-flow rate on blade and cooling-air temperatures for blade 14 at 10,000 rpm.

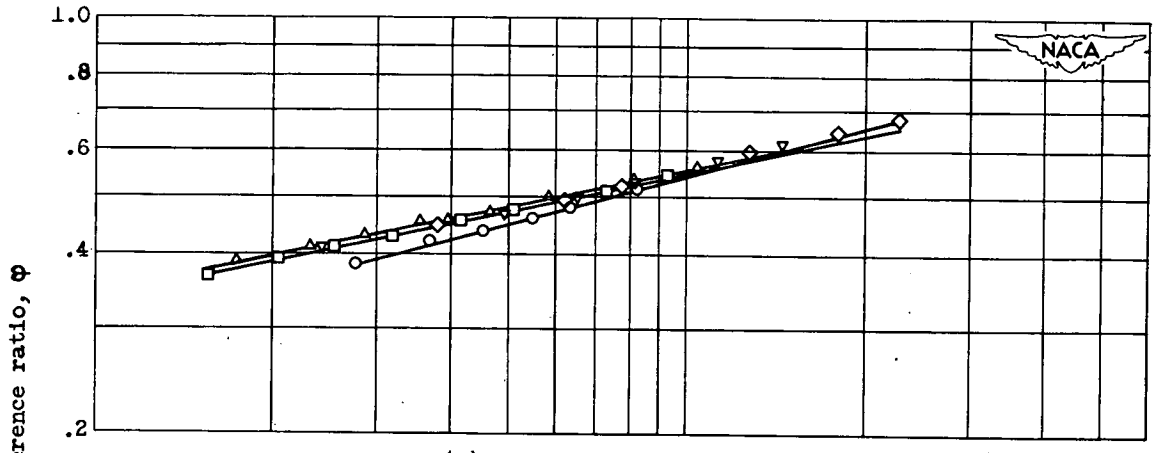

(a) Midchord thermocouple J.

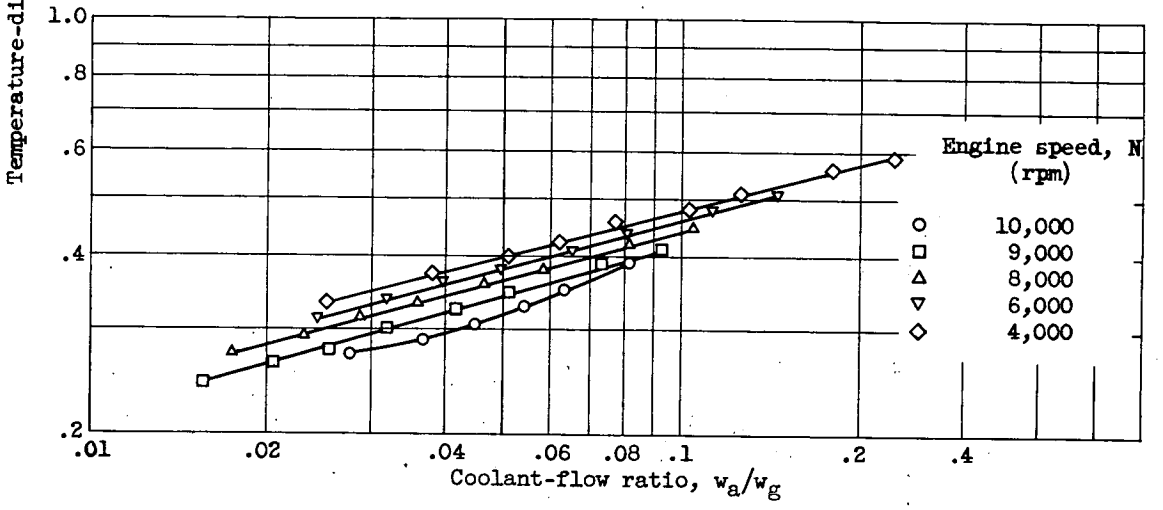

(b) Leading-edge thermocouple G.

Figure 9. - Correlation of blade temperature for blade 11.

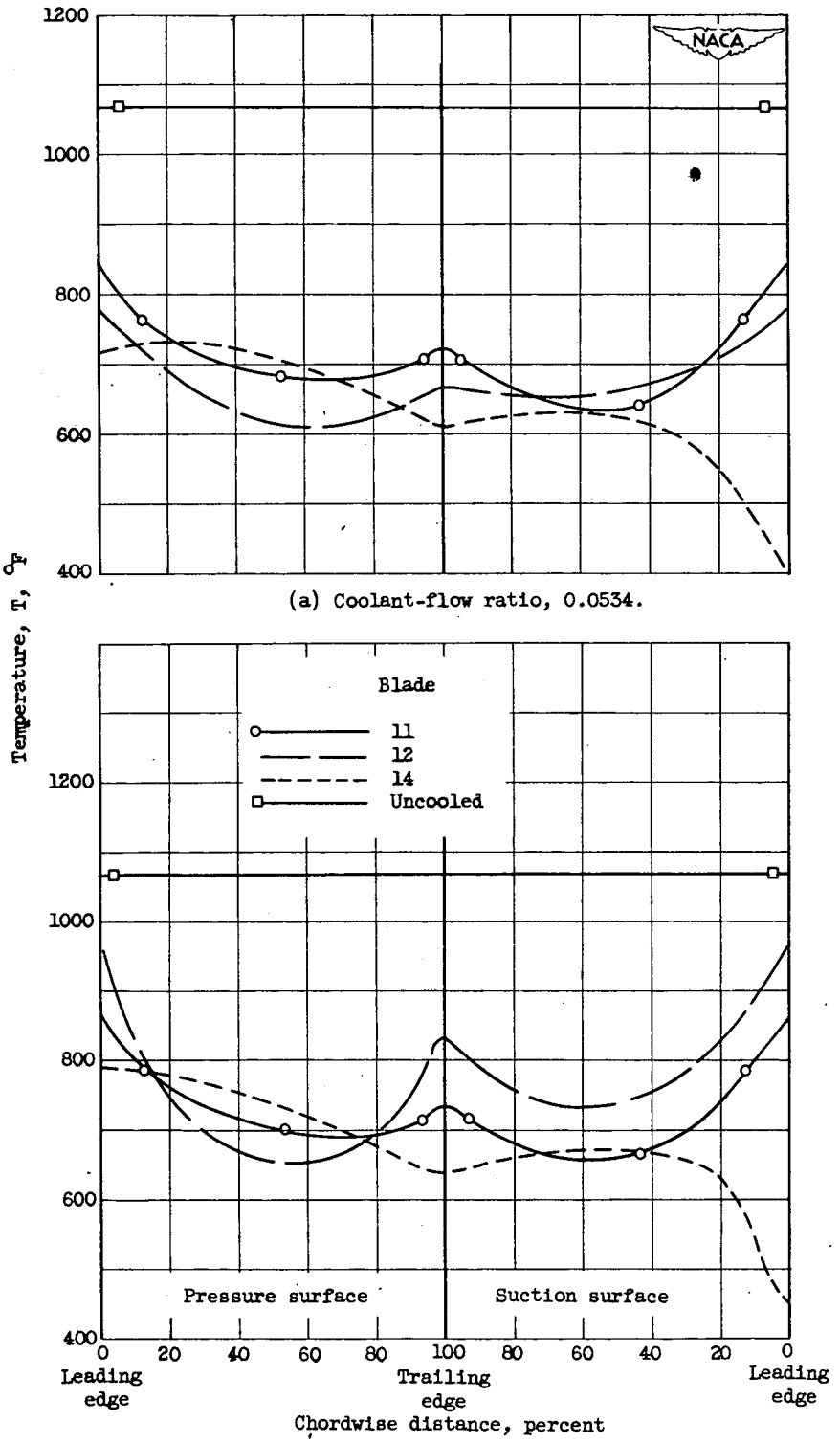

(a) Coolant-flow ratio, 0.0534.

(b) Coolant-flow ratio, 0.045.

Figure 10. - Chordwise temperature comparison of blades investigated. Engine speed, 10,000 rpm; cooling-air inlet temperature, 130° F.

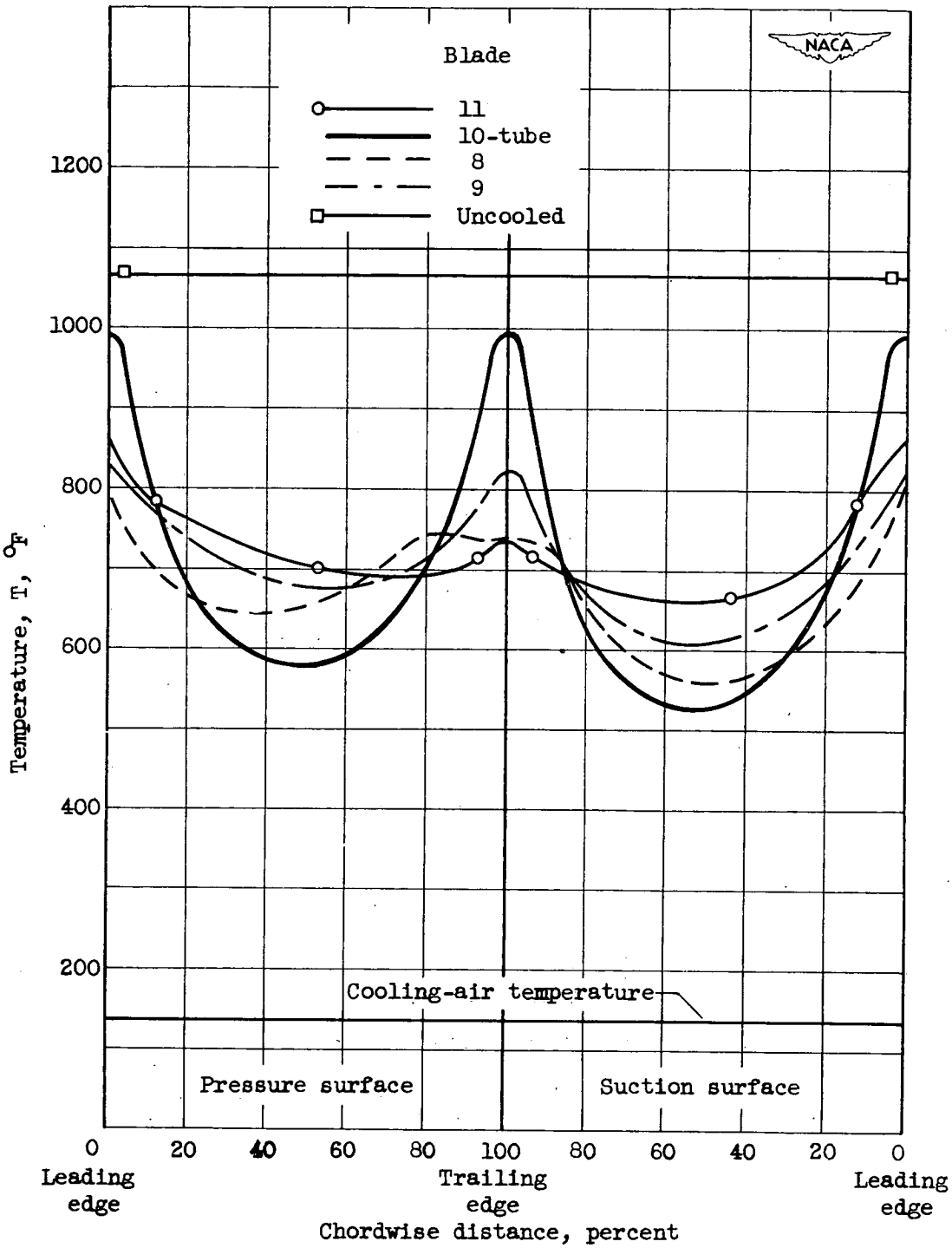

Figure 11. - Chordwise temperature comparison of blade 11 with blades previously investigated. Engine speed, 10,000 rpm; ratio of cooling-air flow to combustion-gas flow, 0.045.

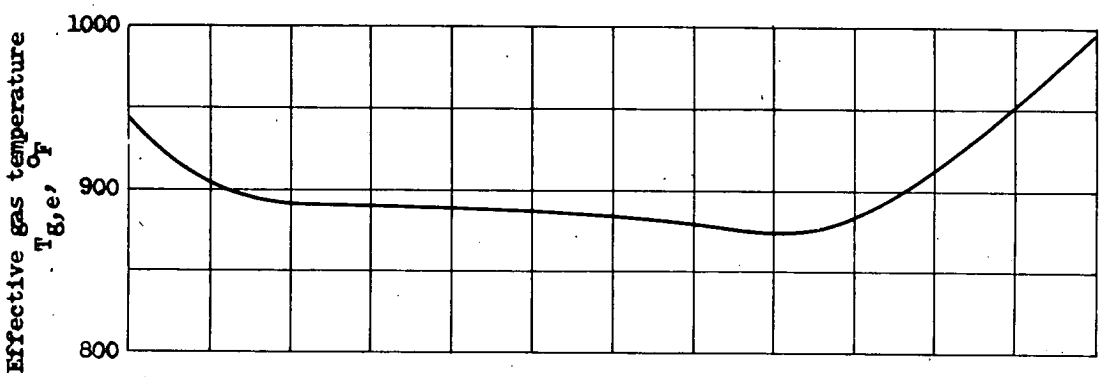

(a) Effective gas temperature.

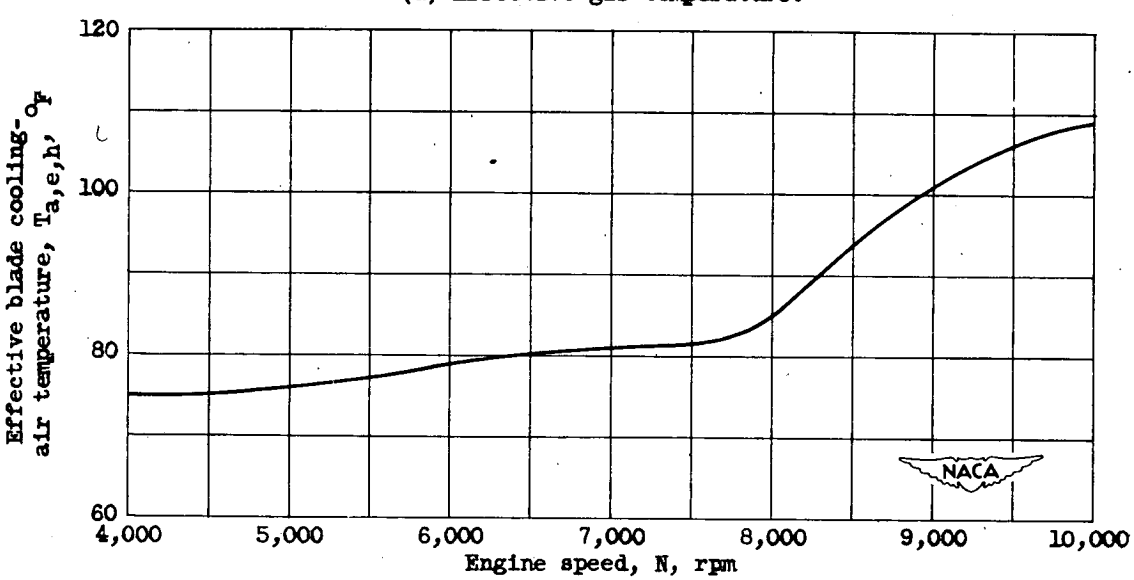

(b) Effective blade cooling-air temperature for coolant-flow ratio of 0.05.

Figure 12. - Variation of effective gas temperature and effective blade cooling-air temperature with engine speed for standard engine-inlet conditions. (Data from fig. 17 of reference 2.)

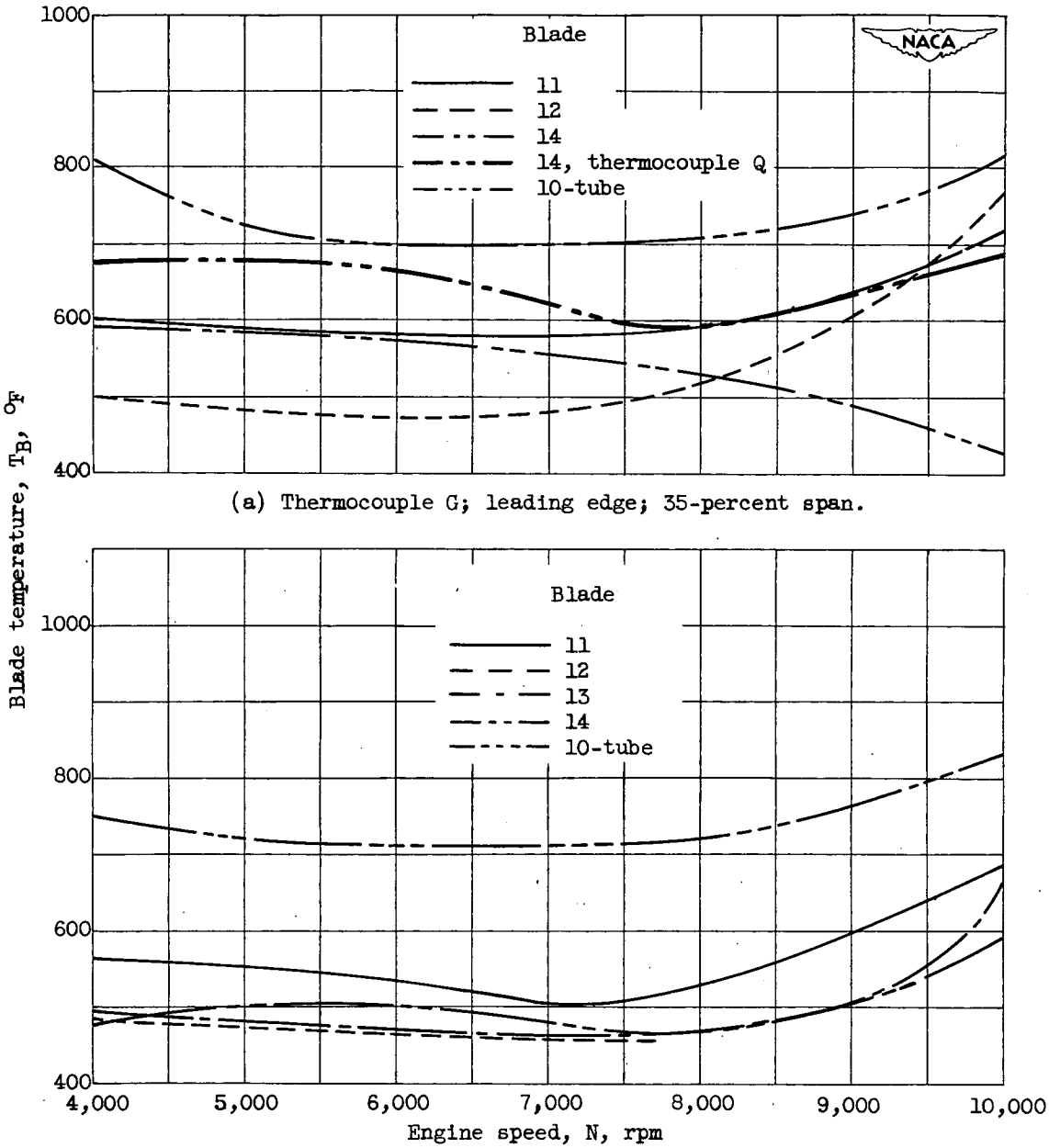

(a) Thermocouple G; leading edge; 35-percent span.

(b) Thermocouple C; trailing-edge; 35-percent span.

Figure 13. - Comparison of temperatures of blades investigated and 10-tube blade over range of engine speeds for standard inlet conditions. Coolant-flow ratio, 0.050.

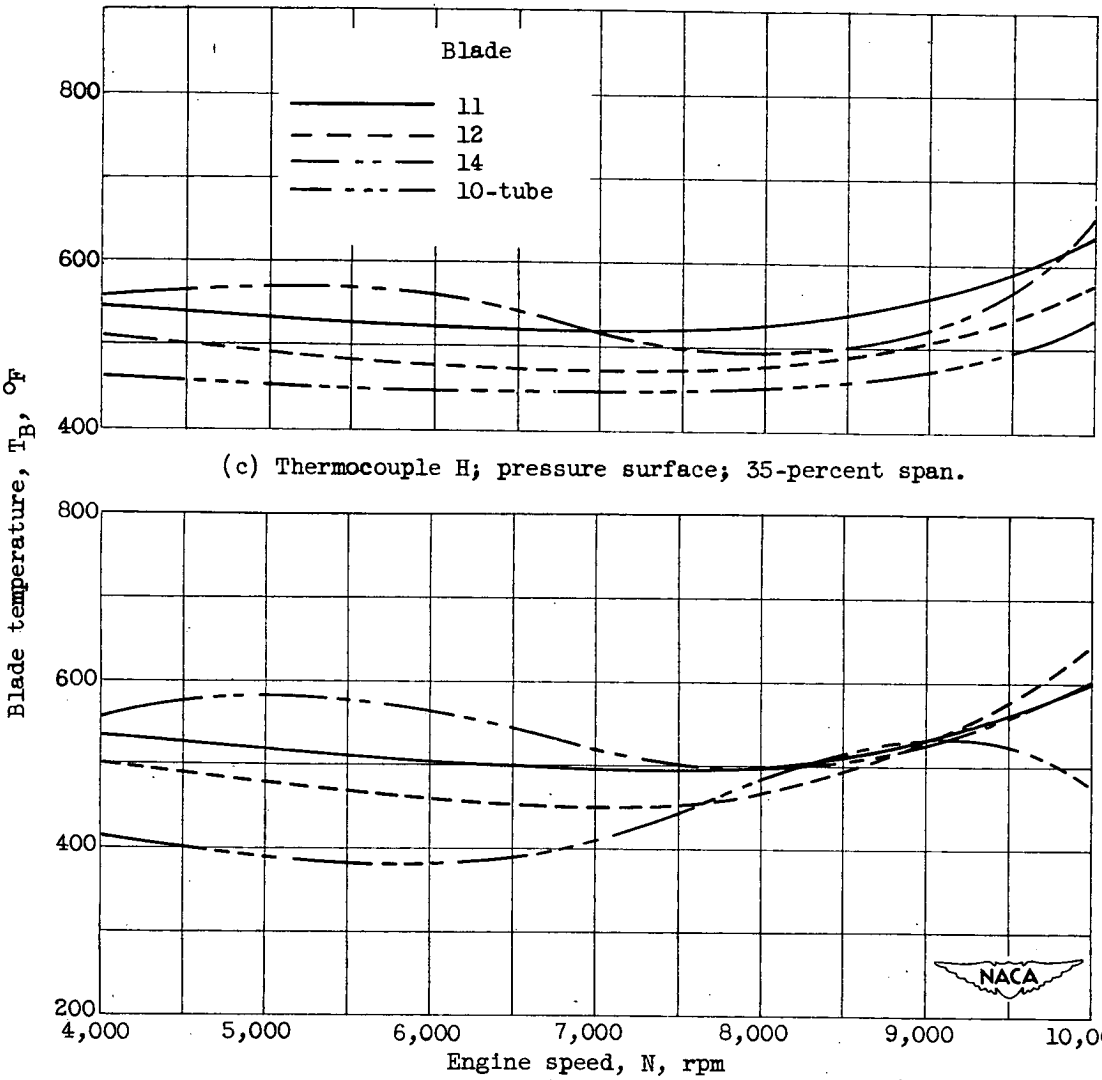

Figure 13. - Concluded. Comparison of temperatures of blades investigated and 10-tube blade over range of engine speeds for standard inlet conditions. Coolant-flow ratio, 0.050.

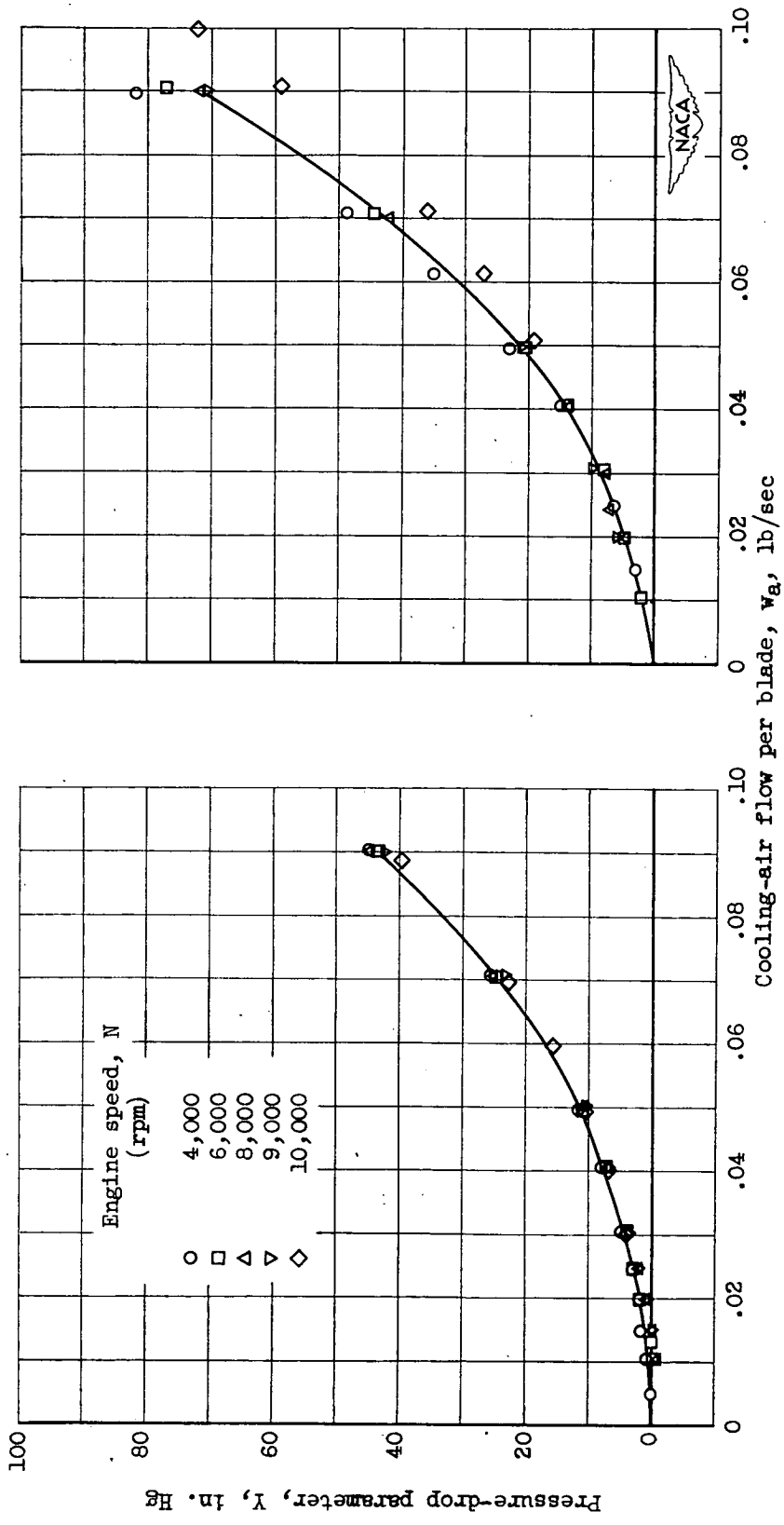

(a) Blade 11.

(b) Blade 12.

Figure 14. - Correlation of cooling-air pressure drop from rotor hub to blade tip.

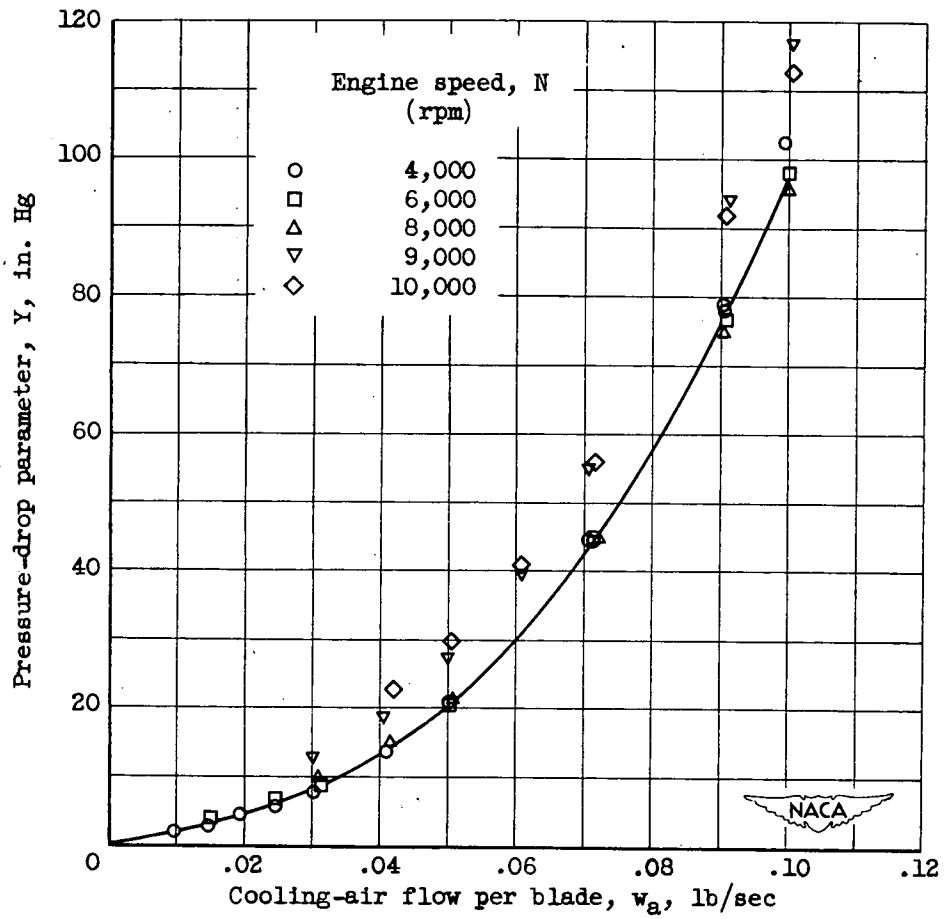

(c) Blade 14.

Figure 14. - Concluded. Correlation of cooling-air pressure drop from rotor hub to blade tip.

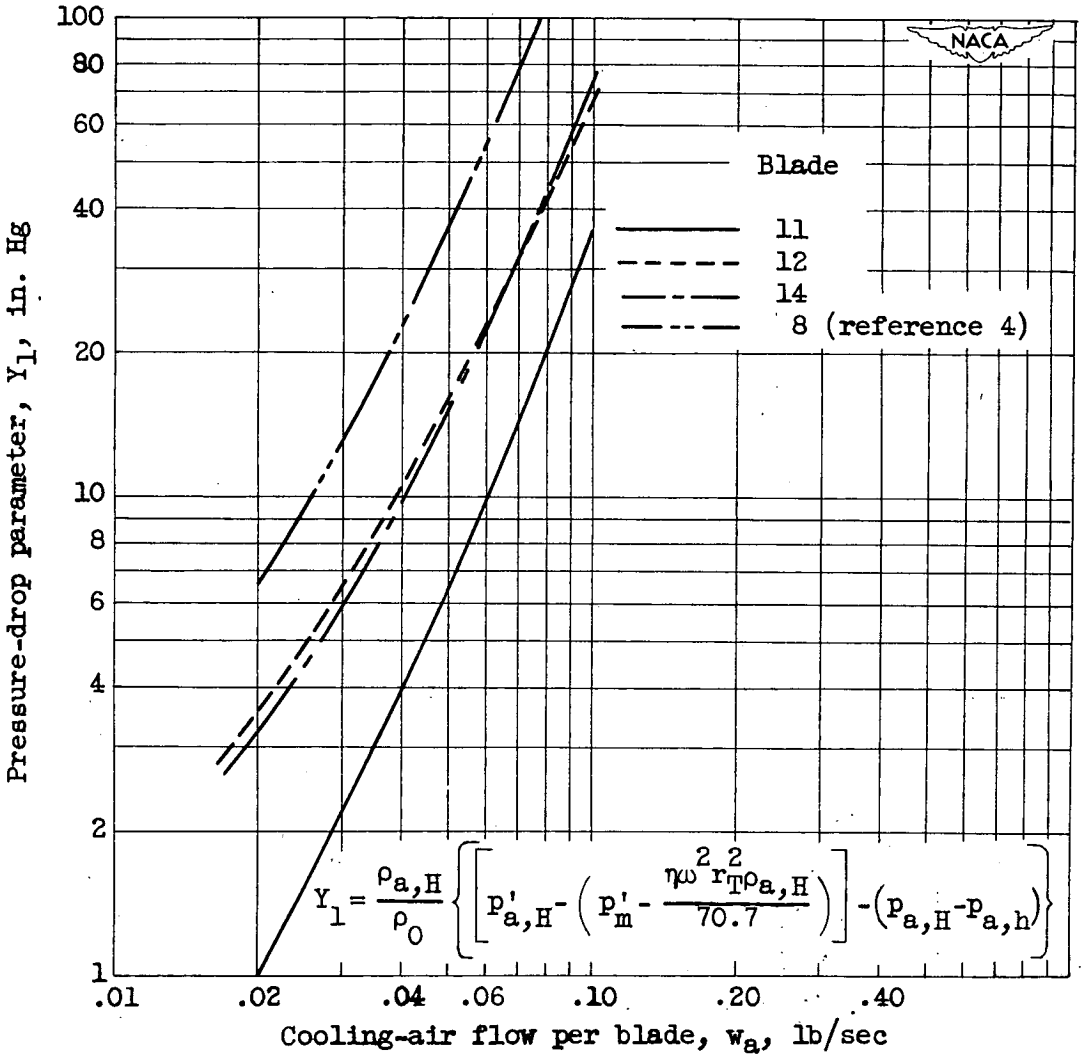

Figure 15. - Comparison of cooling-air pressure drop from root to tip of blades investigated and blade 8.

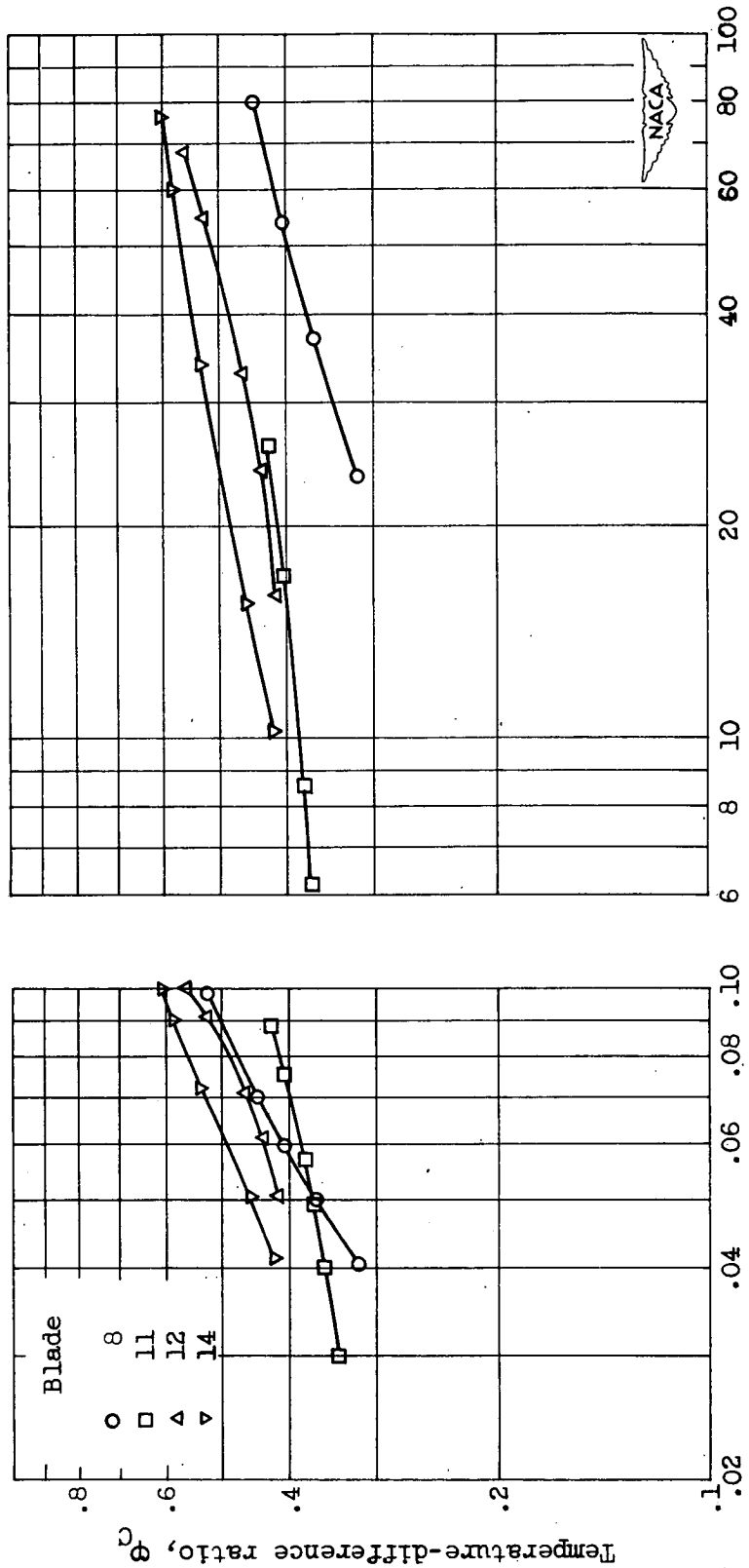

(a) Trailing edge.

Figure 16. - Comparison of blades on basis of cooling effectiveness and blade pressure drop at engine speed of 10,000 rpm.

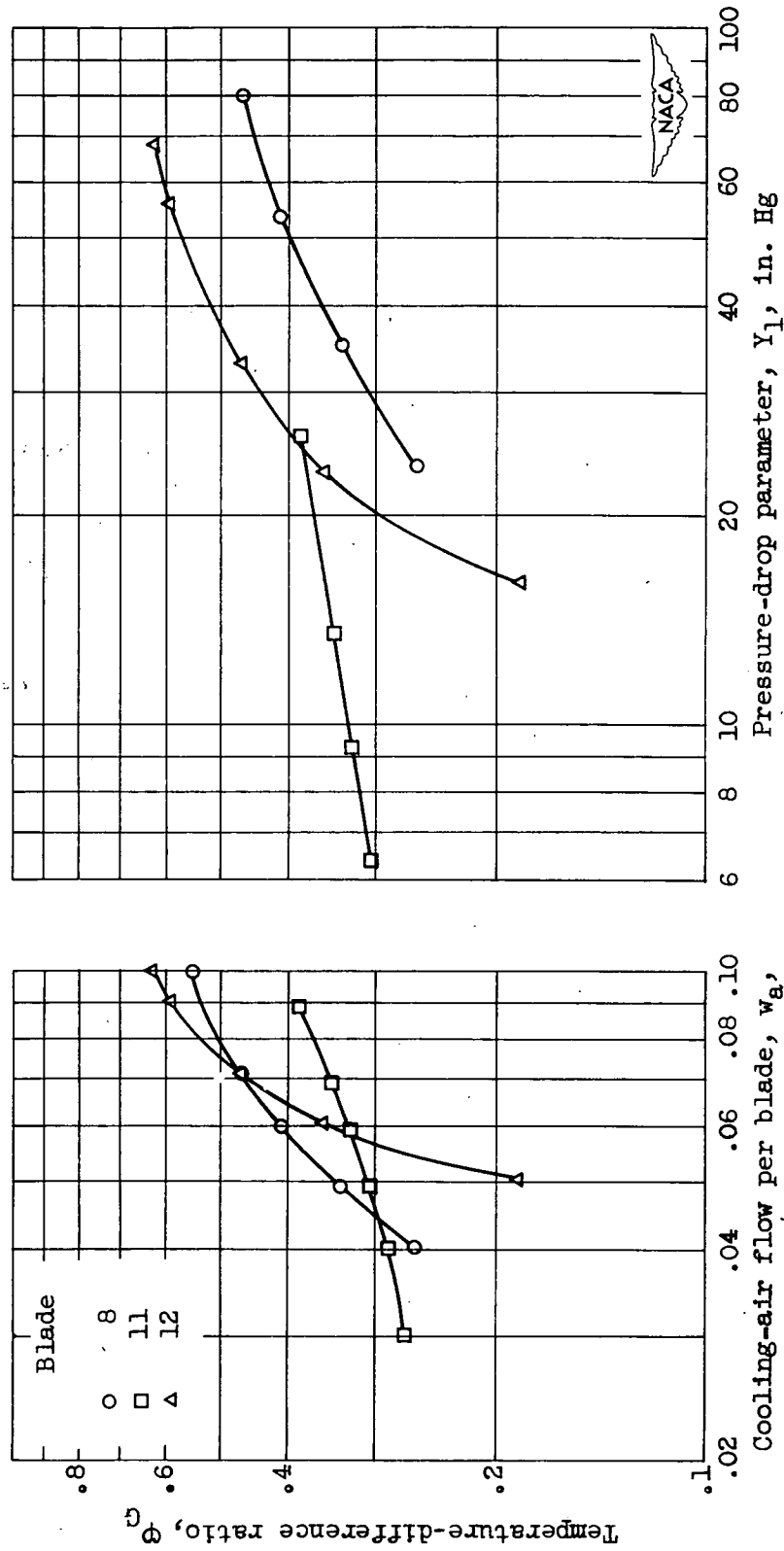

(b) Leading edge.

Figure 16. - Concluded. Comparison of blades on basis of cooling effectiveness and blade pressure drop at engine speed of 10,000 rpm.